"ROLE OF MAGNETIC RESONANCE SPECTROSCOPY IN CENTRAL NERVOUS SYSTEM INFECTIONS – A ONE YEAR HOSPITAL BASED OBSERVATIONAL STUDY"

By

REG NO: BS0119002

Dissertation

Submitted to the
KLE Academy of Higher Education and Research
Belagavi, Karnataka

In partial fulfilment of the requirements for the degree of

DOCTOR OF MEDICINE

IN

RADIO-DIAGNOSIS

DEPARTMENT OF RADIO-DIAGNOSIS

J. N. MEDICAL COLLEGE, BELAGAVI

KARNATAKA, INDIA

APRIL 2022

KLE ACADEMY OF HIGHER EDUCATION AND RESEARCH, BELAGAVI, KARNATAKA

Endorsement by the HOD/Principal/ Head of the Institution

This is to certify that the dissertation entitled **"ROLE OF MAGNETIC RESONANCE SPECTROSCOPY IN CENTRAL NERVOUS SYSTEM INFECTIONS – A ONE YEAR HOSPITAL BASED OBSERVATIONAL STUDY"** is a bonafide research work done by **REG NO.BS0119002.**

Dr. Ashwin S. Patil MD,
Professor and Head,
Department of Radio Diagnosis,
J. N. Medical College,
Nehru Nagar, Belagavi – 10

Date:
Place: Belagavi

Dr. N. S. Mahantshetti MD
Principal,
J. N. Medical College,
Nehru Nagar,
Belagavi – 10

Date:
Place: Belagavi

KLE ACADEMY

ANTI - PLAGIARISM CHECK-ACCEPTANCE LETTER

JAWAHARLAL NEHRU MEDICAL COLLEGE

(Recognized by Medical Council of India, New Delhi)

Accredited 'A' Grade by NAAC (2nd Cycle) Placed in Category 'A' by MHRD (GoI)

Nehru Nagar, Belagavi- 590 010, Karnataka, INDIA

0831 - 2471350 0831 - 2470759 www.jnmc.edu principal@jnmc.edu

Ref No: MDC/PG/ Date: 25-11-2021.

ACCEPTANCE LETTER

The softcopy of thesis entitled: **"ROLE OF MAGNETIC RESONANCE SPECTROSCOPY IN CENTRAL NERVOUS SYSTEM INFECTIONS - ONE YEAR HOSPITAL BASED OBSERVATIONAL STUDY."** has been submitted for Anti-Plagiarism check through Turnitin software. The scan has been carried out and the scanned output reveals a match percentage of **01%** which is within the acceptable limits of **10%** as per the guidelines given by UGC.

Dr. (Mrs.) N.S. Mahantashetti.
Chairperson-Antiplagiarism Committee &
Principal,
J. N. Medical College, Belagavi.

To,
Reg. No. BS0119002.
Postgraduate Student,
2019-20 Batch,
Department of Radiodiagnosis,
J. N. Medical College, Belagavi.

LIST OF ABBREVIATIONS

ADC	–	Apparent diffusion coefficient
Ala	–	Alanine
CISS	–	Constructive interface steady state
Cho	–	Choline
CNS	–	Central nervous system
CT	–	Computed tomography
DWI	–	Diffusion weighted imaging
FID	–	Free induction delay
FLAIR	–	Fluid attenuated inversion recovery
Glu	–	Glutamine
Glx	–	Glutamine-glutamate-GABA complex
HIV	–	Human immunodeficiency virus
JC	–	John Cunnigham
Lac	–	Lactate
Lip	–	Lipid
mI	–	Myoinositol
MRI	–	Magnetic Resonance Imaging
MRS	–	Magnetic resonance spectroscopy
MTR	–	Magnetic transfer imaging
NAA	–	N-Acetyl aspartate
NCC	–	Neurocysticercosis
PML	–	Progressive multifocal leukoencephalopathy
PMRS, 1HMR	–	Proton magnetic resonance spectroscopy
PRESS	–	Point resolved spectroscopy

RF	–	Radiofrequency
STEAM	–	Stimulated echo acquisition mode
SWI	–	Susceptibility Weighted Imaging
SVS	–	Amino acid
Suc	–	Succinate
TBM	–	Tuberculous meningitis
TE	–	Time to echo
TDI	–	Time domain information
TR	–	Repetition time
TB	–	Tuberculosis
VZE	–	Varicella zoster encephalitis

ABSTRACT

INTRODUCTION

Since the advent of MRI, it has become the modality of choice for diagnosis of CNS infections. However, its role was limited to the morphological evaluation of the brain. With MR spectroscopy, it is possible to get an insight to the metabolic composition of the lesion. Spectroscopy is currently used in diagnosis of CNS infections, CNS neoplasms and various metabolic disorders.

MR spectroscopy can point to a specific etiology of CNS infection which can reduce the need of unnecessary procedures and treatments and can lead to early diagnosis and initiation of early treatment.

OBJECTIVES:

1. Assess the diagnostic value and accuracy of magnetic resonance spectroscopy for differentiating various central nervous system infections
2. Correlation of metabolic peaks and ratios obtained via magnetic resonance spectroscopy with various central nervous system infections and assessing their diagnostic value

MATERIAL AND METHODS:

The current study was a prospective observational study, conducted in the Dr.Prabhakar Kore hospital and MRC, KLE University, Belgaum between January 2020 and December 2020 for a period of 1 year in 48 patients having CNS infections. All the study participants were referred to the Radio-diagnosis department for MRI of the brain by their respective clinicians.

All the 48 patients underwent routine MR brain screening including T1, T2, FLAIR and Diffusion weighted sequences. Additional sequences like contrast and spectroscopy were done in patients with suspected CNS infections. The routine MR and spectroscopy findings were then correlated with the clinical diagnosis.

RESULTS

Our study included evaluation of 48 patients which included: 27 males and 21 females with mean age of 44.2 years. The lesions were evaluated on the basis of number, location, morphological features, T1, T2, DWI and T1 post contrast findings. MR Spectroscopy was used to correlate the relevant level of metabolic peaks and their ratios in every individual case with the clinical diagnosis of the patient.

INTERPRETATIONS AND CONCLUSIONS

This study aimed at correlating the MRI and spectroscopy findings with the clinical diagnosis. In our study most of the CNS infections presented as T1 variable and T2 hyperintense lesions which showed ring enhancement. DWI showed variable results depending on the morphology of the lesion. The spectroscopy showed predominant amino acid and lactate peaks in bacterial abscesses and few of the fungal abscesses showed Trehalose peaks. Few of the abscesses showed an increased A/S ratio suggestive of anaerobic microbia. Lipid-lactate peaks were the predominant finding in most of the tuberculomas and few of the abscesses. Reduced NAA was also seen in bacterial abscesses, tuberculoma, toxoplasmosis, PML, NCC and cryptococcoma, however decrease in NAA/Cr was a relatively specific finding for cerebritis and HIV/HSV Encephalitis. Spectroscopy was normal in few of the cases.

The study concludes that MR spectroscopy can be crucial to supplement the MRI findings to establish a confident diagnosis of the specific etiology of a CNS infection.

KEYWORDS

Magnetic resonance spectroscopy (MRS), Magnetic resonance imaging (MRI), CNS infections

CONTENTS

LIST OF FIGURES

LIST OF TABLES

LIST OF GRAPHS

LIST OF MRI CASE IMAGES

INTRODUCTION

Since the advent of magnetic resonance (MR) imaging, its importance in the diagnosis of the central nervous system (CNS) pathologies has undergone a major overhaul. Previously unprecedented detailed imaging of the CNS is now made possible with the proton signal of water. Various basic sequences in MRI (T1, T2 and FLAIR) and advanced sequences (DWI, Perfusion, SWI and Spectroscopy) provides availability of detailed structural, functional and molecular information plays an invaluable role for the neuro-radiologist for diagnosis of pathologies like stroke, hemorrhage, malignancies and infections.

Although detailed knowledge is commonly available on possible findings in every infection, there is significant overlap of the imaging characteristics in few of the CNS infections.[1]

Central nervous system (CNS) infections includes meningitis, encephalitis, and brain abscess, are rare but time-sensitive emergency department (ED) diagnoses.[2]

CNS infections present with a wide range of findings in MR imaging; however the presentation can show some overlap. It becomes essential to correlate with laboratory testing, particularly cerebro-spinal fluid (CSF) analysis, to establish a definitive diagnosis.

According to a study conducted by Rantakallio P, Leskinen M, von Wendt L, the incidence of bacterial CNS infections was 36 per 100,000 while that of viral infections 688 per 100000 per annum. Another study by Kumar D, Pannu AK, Dhibar DP, Singh R, Kumari S, CNS tuberculosis was the most common cause (51 %) of CNS infection, viral meningoencephalitis (13 %), community-acquired bacterial meningitis (9 %), cryptococcal meningitis (6 %), scrub typhus meningo-encephalitis (1%), fungal brain abscesses (1 %) and neurocysticercosis (NCC) (1 %). [3]

Complementary to structural MR imaging, proton magnetic resonance spectroscopy (MRS) has become a different approach to assess the metabolite level in normal or

diseased neuroparenchyma, especially as image-controlled, localized MR spectroscopy acquisition techniques are developed. The early localization techniques included Stimulated Echo Acquisition Mode (STEAM) and Point Resolved Spectroscopy (PRESS) techniques that are now widely prevalent in clinical MR spectroscopy application. [4]

The ability to make an early, noninvasive diagnosis or to increase confidence in a suspected diagnosis is highly valued by patients and clinicians alike. As a result, MR spectroscopy is rapidly being incorporated into the scan protocols for brain examinations in indicated patients. MR spectroscopy combined with routine diagnostic MR imaging, can provide specific information which may help in a more confident diagnosis. However, it may have a supportive role in the diagnosis and follow up of other CNS infections.

MR Spectroscopy quantitates the tissue metabolites such as NAA, creatine, choline, and lactate etcetera and the information is correlated with differentials to establish diagnosis. Single-voxel spectroscopy (SVS) and multi-voxel spectroscopy are two different techniques to perform the scan.

The presence of lactate peak suggests necrotic areas within the lesion. The presence of amino acids can suggest bacterial abscesses. The acetate/succinate ratio differentiates parasitic from the pyogenic infections. A sugar named Trehalose is very specific for fungal etiology. Magnetic resonance spectroscopy is diagnostic in pyogenic abscesses and parasitic infections. Two-dimensional magnetic resonance spectroscopic imaging (MRSI) can be helpful in differentiating between abscess and necrotic tumors. Proton MRS provides information to understand the exact biochemical composition of the CNS lesion and the physiological changes that occur in the adjacent parenchyma. Cohort studies have demonstrated that Proton MRS has proven useful in monitoring the progression of a disease and response to treatment. MR spectroscopy also has a prognostic implication.[5]

Therefore, our study mainly focuses on assessing the accuracy of MR spectroscopy in aiding the diagnosis of CNS infections and characterizing the molecular constituents and molecular ratios of various CNS infections.

OBJECTIVES

1. Assess the diagnostic value and accuracy of magnetic resonance spectroscopy for differentiating various central nervous system infections
2. Correlation of metabolic peaks and ratios obtained via magnetic resonance spectroscopy with various central nervous system infections and assessing their diagnostic value

REVIEW OF LITERATURE

EMBRYOLOGY OF CENTRAL NERVOUS SYSTEM

The central nervous system (CNS) appears at the beginning of the 3 weeks like a slipper-shaped plate of ectoderm, the neural plate. This plate is located in the dorsal region near the primitive pit. Its lateral edges become elevated and fuse in the midline, thus forming the neural tube.

By the fourth week of gestation, three vesicular dilatations develop in the rostral portion of the neural tube, thereby forming the forebrain (prosencephalon), midbrain (mesencephalon) and hindbrain (rhombencephalon).

By the fifth week of gestation, the developing forebrain has divided into a cephalic telencephalon and caudal diencephalon. The hindbrain is divided into a cephalic metencephalon and caudal myelencephalon. The metencephalon forms the pons and cerebellum while the myelencephalon forms the medulla oblongata.

Bilateral diverticula from the telencephalic portion of the neural tube form cerebral hemispheres. These hemispheres undergo expansion and folding with formation of permanent primitive fissures by the $4th$ month. There are three major flexures which are the midbrain, pontine and cervical flexures. They divide the developing brain into the cerebrum, cerebellum and spinal cord.

The central hemispheres are smooth surfaced (lissencephalic) in early development, and a germinal matrix of primitive cells surrounds each lateral ventricle. Embryonal tissue from the germinal matrix proliferates, migrates outward towards the cortex and mature as neuroglial cells. The germinal matrix is formed at 7 weeks and involutes at 28 to 30 works,

although it persists in the form of focal cell clusters in week 36 through 39. During the sixth and seventh gestational months, the cerebral surfaces convolute to form primitive gyri and sulci. The adult neuroparenchyma pattern may already be recognizable towards the end of gestation. Along with cortical development, the formation of fiber acts occurs, including the commissures between the two cerebral hemispheres.

NORMAL ANATOMY

Brain parenchyma, meninges, cranial nerves and CSF form the contents of the cranial cavity. The anatomy of the head is studied in the form of cross-sectional images in axial, sagittal and coronal planes.

CEREBELLAR HEMISPHERES

The falx cerebri and interhemispheric fissure separates the two cerebral hemispheres. Each cerebral hemisphere consists of outer gray matter (cerebral cortex) and inner white matter.

Both hemispheres are divided into five lobes: frontal, parietal, temporal, occipital and insula (central lobes). The central fissure separates the frontal lobe from the parietal lobe. Laterally, the sylvian fissure separates the frontal lobe from the temporal lobe.

Corpus callosum is a central white matter commissure that connects both of the cerebral hemispheres. Corpus callosum is made of Genu, Body, Splenium and Rostrum. Basal ganglia represents the central gray matter. It consists of caudate nuclei, lentiform (globus pallidus and putamen) nucleus, claustrum and amygdala. The internal capsule is a boomerang shaped white matter is made of anterior limb, genu and posterior limb. The centrum semiovale makes up the white matter of the cerebral hemispheres.

The diencephalon is made up of thalami, geniculate bodies, epithalamus, subthalamus and hypothalamus

BRAIN STEM

Brain stem is formed by the midbrain, pons and the medulla. Midbrain is the cranial most part of the brain stem, which forms the connecting link between the forebrain and hindbrain. It consists of the ventral portion called cerebral peduncle and a smaller dorsal portion called tectum.

The triangle-shaped space between the two cerebral peduncles forms the interpeduncular fossa. The tectum is made of four round projections called corpora quadrigemina. The pons connects with the midbrain superiorly and medulla inferiorly. The module is the most inferior part of the brain stem and connects to the cervical spinal cord. At the level of foramen magnum it contains the posterior median sulcus and anterior median fissure.

CEREBELLUM

Cerebellum occupies the posterior cranial fossa. It is situated posterior to the pons and is separated from the pons and medulla by the 4^{th} ventricle. The cerebellum consists of two hemispheres, which are joined in the midline by vermis.

CSF SPACES

The CSF is mainly produced by the granulations of the choroid plexus which is situated in bilateral lateral ventricles. There are two lateral ventricles, third and fourth ventricles. The lateral ventricles communicate through the interventricular foramina with the 3^{rd} ventricle. The 3^{rd} ventricle is connected to the 4^{th} ventricle by an aqueduct of Sylvius. The 4^{th}

ventricle connects with the canal of the spinal cord and the foramen of Magendie and Luschka drains into the subarachnoid cisterna.

CRANIAL NERVES

There are twelve pairs of cranial nerves. It is possible to identify the intracranial portions of the cranial nerves using MRI, especially with the help of CISS sequence.

VASCULAR SYSTEM

The two internal carotid and vertebral arteries supply the supra and infratentorial neuroparenchyma. These four arteries course within the subarachnoid spaces, and their branches anastomose in the middle cranial fossa (MCF) to form the circle of Willis. The circle of Willis is formed by anterior communicating, ACA, ICA, posterior communicating, PCA and basilar arteries contribute to the formation of the

The circle of Willis enables the blood that enters in either internal carotid artery or vertebral arteries to be perfused to any portion of bilateral cerebral hemispheres. The cerebral venous system is composed of venous sinuses in the dural space, cortical, deep medullary and subependymal veins.

DURA AND DURAL STRUCTURES

The brain is covered by 3 layers of meninges- pia mater, arachnoid membrane and dura mater. The pia mater is adherent to all the gyri with the arachnoid membrane overlying it. The dura mater is separated from the arachnoid membrane by subdural space. The outer layer of the dura is attached to the periosteum of the bony calvarium. The inner layer of the dura forms infolding within the cranial vault. The two major folds are falx cerebri and tentorium cerebelli.

MRI SEQUENCES – BASICS AND DIFFERENCES:

Magnetic resonance imaging is the best imaging modality for imaging of the brain and spine. Quality of the received images depends on many technical factors like positioning of the patient, proper coil selection, selection of appropriate sequences and image planes. MRI has the advantage of visualizing anatomy in all three planes: axial, sagittal and coronal. In comparison with CT, it can detect flowing blood and cryptic vascular malformations. It can also detect demyelinating disease, and has no beam-hardening artifacts such as can be seen with CT. Thus, the posterior fossa is more easily visualized on MRI than CT. Imaging is also performed without any ionizing radiation.

MRI is based on the magnetization properties of atomic nuclei. A powerful, uniform, external magnetic field is employed to align the protons that are normally randomly oriented within the water nuclei of the tissue being examined.[6,7,8]

This alignment (or magnetization) is next perturbed or disrupted by introduction of an external Radio Frequency (RF) energy. The nuclei return to their resting alignment through various relaxation processes and in so doing emit RF energy. After a certain period following the initial RF, the emitted signals are measured. Fourier transformation is used to convert the frequency information contained in the signal from each location in the imaged plane to corresponding intensity levels, which are then displayed as shades of gray in a matrix arrangement of pixels. By varying the sequence of RF pulses applied & collected, different types of images are created. [9,10]

Repetition Time (TR) is the amount of time between successive pulse sequences applied to the same slice.

Time to Echo (TE) is the time between the delivery of the RF pulse and the receipt of the echo signal.

Tissue can be characterized by two different relaxation times – T1 and T2.

T1 (longitudinal relaxation time) is the time constant which determines the rate at which excited protons return to equilibrium. It is a measure of the time taken for spinning protons to realign with the external magnetic field.

T2 (transverse relaxation time) is the time constant which determines the rate at which excited protons reach equilibrium or go out of phase with each other. It is a measure of the time taken for spinning protons to lose phase coherence among the nuclei spinning perpendicular to the main field.[11,12]

The various MRI sequences are:

1. T1 weighted image

2. T2 weighted image

3. Diffusion Weighted Imaging

4. Fluid Attenuation Inversion Recovery

5. Susceptibility Weighted Imaging

6. Apparent Diffusion Coefficient

7. Magnetic Resonance Spectroscopy

The most common MRI sequences are T1-weighted and T2-weighted scans. T1-weighted images are produced by using short TE and TR times. The contrast and brightness of the image are predominantly determined by T1 properties of tissue. Conversely, T2-weighted images are produced by using longer TE and TR times. In these images, the contrast and brightness are predominantly determined by the T2 properties of tissue.

In general, T1- and T2-weighted images can be easily differentiated by looking at the CSF. CSF is dark on T1-weighted imaging and bright on T2-weighted imaging.

A third commonly used sequence is the Fluid Attenuated Inversion Recovery (Flair). The Flair sequence is similar to a T2-weighted image except that the TE and TR times are very long. By doing so, abnormalities remain bright but normal CSF fluid is attenuated and made dark. This sequence is very sensitive to pathology and makes the differentiation between CSF and an abnormality much easier.

T1-weighted imaging can also be performed while infusing Gadolinium (Gad). Gad is a non-toxic paramagnetic contrast enhancement agent. When injected during the scan, Gad changes signal intensities by shortening T1. Thus, Gad is very bright on T1-weighted images. Gad enhanced images are especially useful in looking at vascular structures and breakdown in the blood-brain barrier [e.g., tumors, abscesses, inflammation (herpes simplex encephalitis, multiple sclerosis, etc.].

Diffusion weighted imaging (DWI) is designed to detect the random movements of water protons. Water molecules diffuse relatively freely in the extracellular space; their movement is significantly restricted in the intracellular space. Spontaneous movements, referred to as diffusion, rapidly become restricted in ischemic brain tissue. During ischemia, the sodium - potassium pump shuts down and sodium accumulates

intracellularly. Water then shifts from the extracellular to the intracellular space due to the osmotic gradient. As water movement becomes restricted intracellularly, this results in an extremely bright signal on DWI. Thus, DWI is an extremely sensitive method for detecting acute stroke.

Difference between T1 weighted, T2 weighted and FLAIR sequences

Tissue	T1-Weighted	T2-Weighted	Flair
TR	Short TR	Long TR	Very long
TE	Short TE	Long TE	Very long
CSF	Dark	Bright	Dark
White Matter	Light	Dark Gray	Dark Gray
Cortex	Gray	Light Gray	Light Gray
Fat inside bone marrow	Bright	Light	Light
Inflammation (infection, demyelination)	Dark	Bright	Bright

The neurological indications for cranial MRI include indications for [13]

1. Infection (abscess, cerebritis, encephalitis, meningitis)
2. Tumor (primary CNS and metastatic)
3. Vascular conditions like ischemic and hemorrhagic stroke, AVM, aneurysm, venous thrombosis
4. Trauma (epidural hematoma, subdural hematoma, contusion)
5. Inflammatory/Demyelinating Lesions (multiple sclerosis, sarcoidosis, etc.)
6. Hydrocephalus, Congenital Malformations and others

Contraindications to MRI include presence of implanted magnetic electronic devices and other metallic devices like pacemakers, artificial heart valves and intraocular metallic foreign bodies. Pregnancy is a relative contraindication due to unknown effects on the fetus.

MRI sequences also have some disadvantages. They are subject to motion artifacts and require prolonged acquisition time for many images. They are inferior to CT in detecting acute hemorrhage and bony injuries.

Fig.1.NORMAL MRI BRAIN IMAGES

Fig 1a.T1 AXIAL

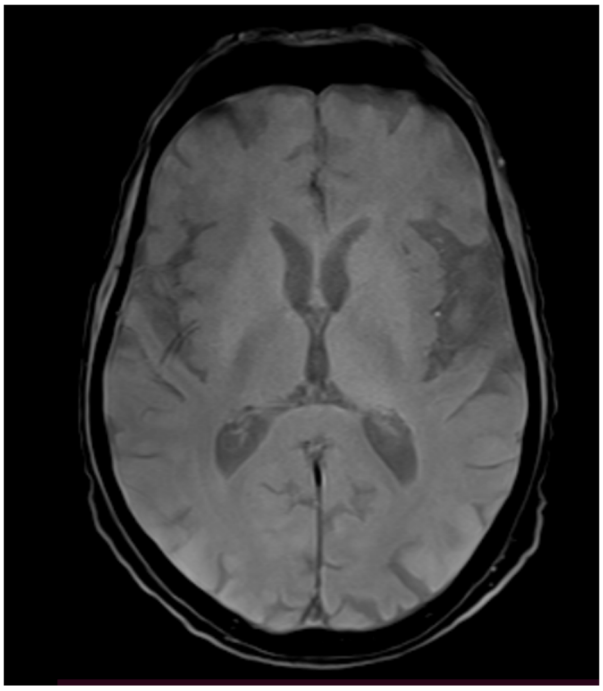

Fig.1b.T2 AXIAL

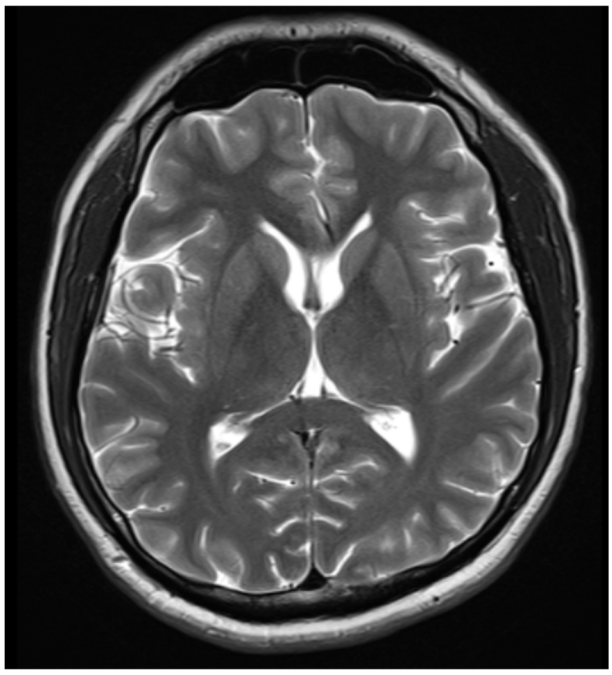

Fig.1c.FLAIR AXIAL

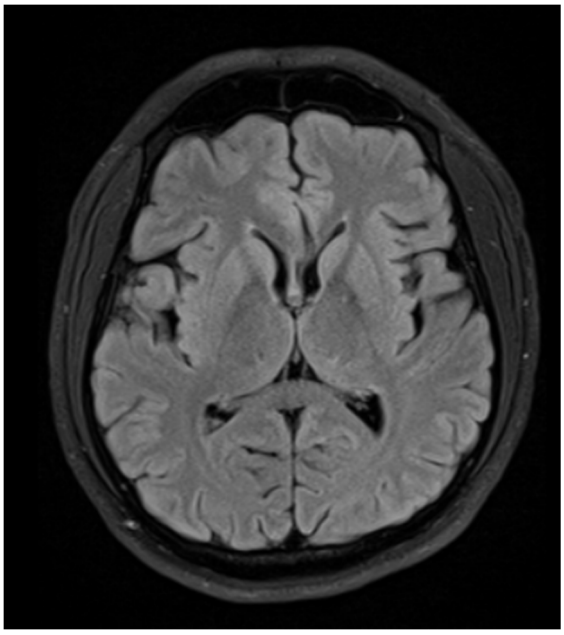

Fig.1d.T1 FS POST CONTRAST AXIAL

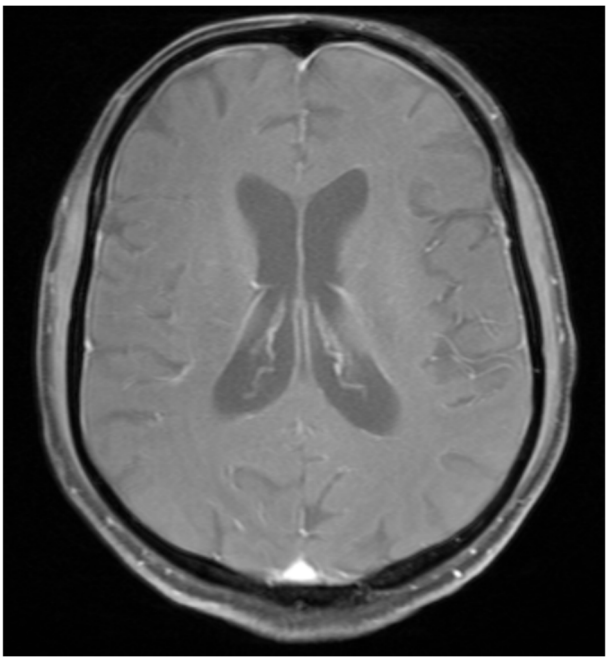

MAGNETIC RESONANCE SPECTROSCOPY

Magnetic resonance spectroscopy (MRS) is a means of non-invasive imaging of the brain. It measures absolute and relative levels of different brain tissue metabolites. In MRI, the time domain information [FID] of free induction decay signals are used to obtain information about the nuclear relaxation time, namely T1 and T2, which are processed to generate anatomic pictures. In MR Spectroscopy, time domain information [TDI] is converted to frequency domain information [FDI] through Fourier transformation.

Magnetic resonance spectroscopy (MRS) measures the sum of metabolite signals amplitude VS time graph in response to RF excitation very similar to MR imaging. The relative quantity and chemical formula determine the frequency and amplitude of that individual metabolite. The basis of the MR spectroscopy is the chemical shift phenomenon. The position of every metabolite on the graph plot is determined by the chemical composition of the brain tissue. If spectral resolution enhances, there is narrowing of chemical shifts predominantly in singlets or splitting into doublet, triplet, and other multiplet due to a spin -spin coupling / J coupling.

MRS can be useful in evaluation of brain tumors and can aid in specific diagnosis of tumors like gliomas, meningioma, lymphoma, oligodendroglioma and astrocytomas. It plays a crucial role in evaluation of autoimmune disorders like Multiple sclerosis and Systemic lupus erythematosus (SLE). MRS has recently shown promising results in the study of psychiatric brain disorders in diseases like bipolar disorders, depression, autism spectrum disorder, schizophrenia and panic disorders. Some studies have revealed correlation between tCho levels in a breast MRI as a marker of malignancy. MRS can also be used to assess breast tumor response to cancer treatment. While doing multiparametric MRI prostate, MRS can be helpful in differentiating adenocarcinoma of prostate and the

healthy tissue. The differentiation is done by calculating the Cho + Cr/citrate ratio which is less than 0.8 in normal prostate and the ratio is more than 0.8 in malignancies.[14]

Apart from MRS, it has a clinical proven role in diagnosis of mitochondrial diseases. Hepatic MR spectroscopy is a new technique that has the potential to improve the accuracy of tissue analysis. Hepatic Proton-MR spectroscopy can be used for the diagnosis of hepatitis, cirrhosis and various cancers.[15]

Fig.2. NORMAL MR SPECTROSCOPY

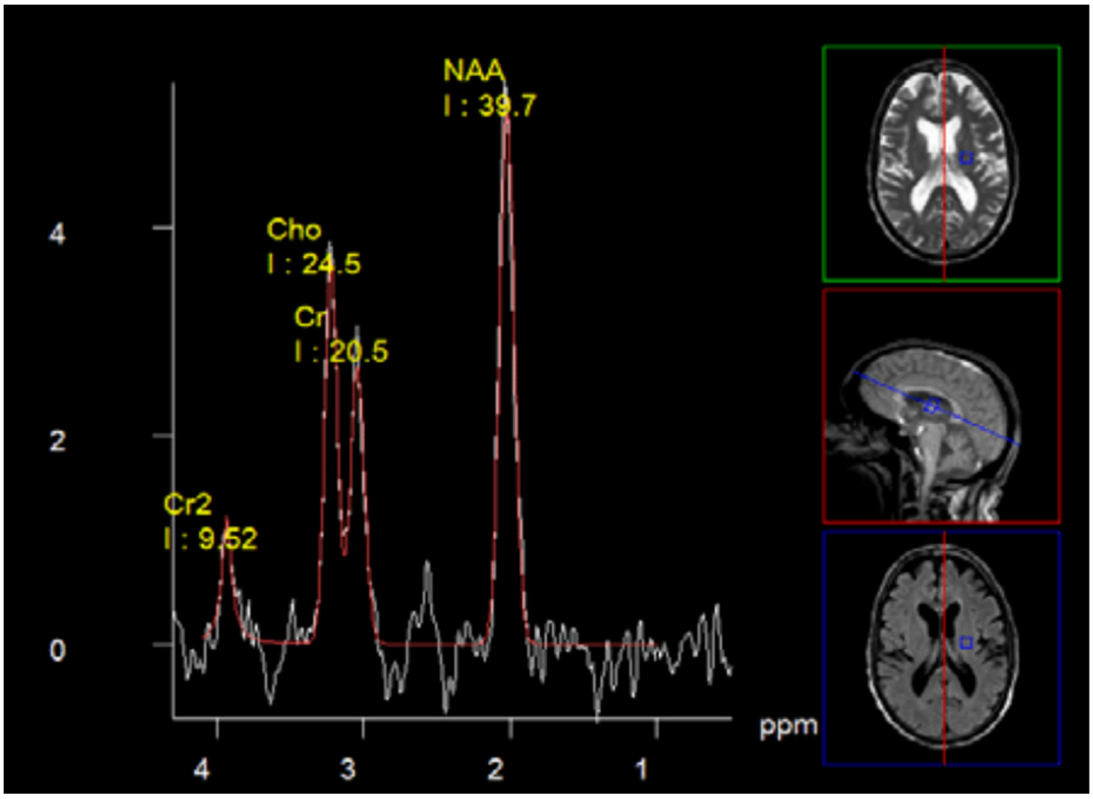

A normal MR spectrum is read right to left with metabolite peaks at various locations on X-axis, lipids appear at 0.9 and 1.3ppm, lactate (doublet peak) appears at 1.3ppm, (NAA) N-acetylaspartate comes at 2.0 ppm, (Cr) creatine appears at 3.0 ppm and (Cho) choline appears at 3.2 ppm and Myo-inositol (mI) appears at 3.6. The line joining ml, Cr, Cho and NAA forms 45 degree with the X-axis if they are present in normal values is labelled as the Hunter's angle.

Hunter's angle changes as we change the echo time and change the repetition time with change in voxel location.[16]

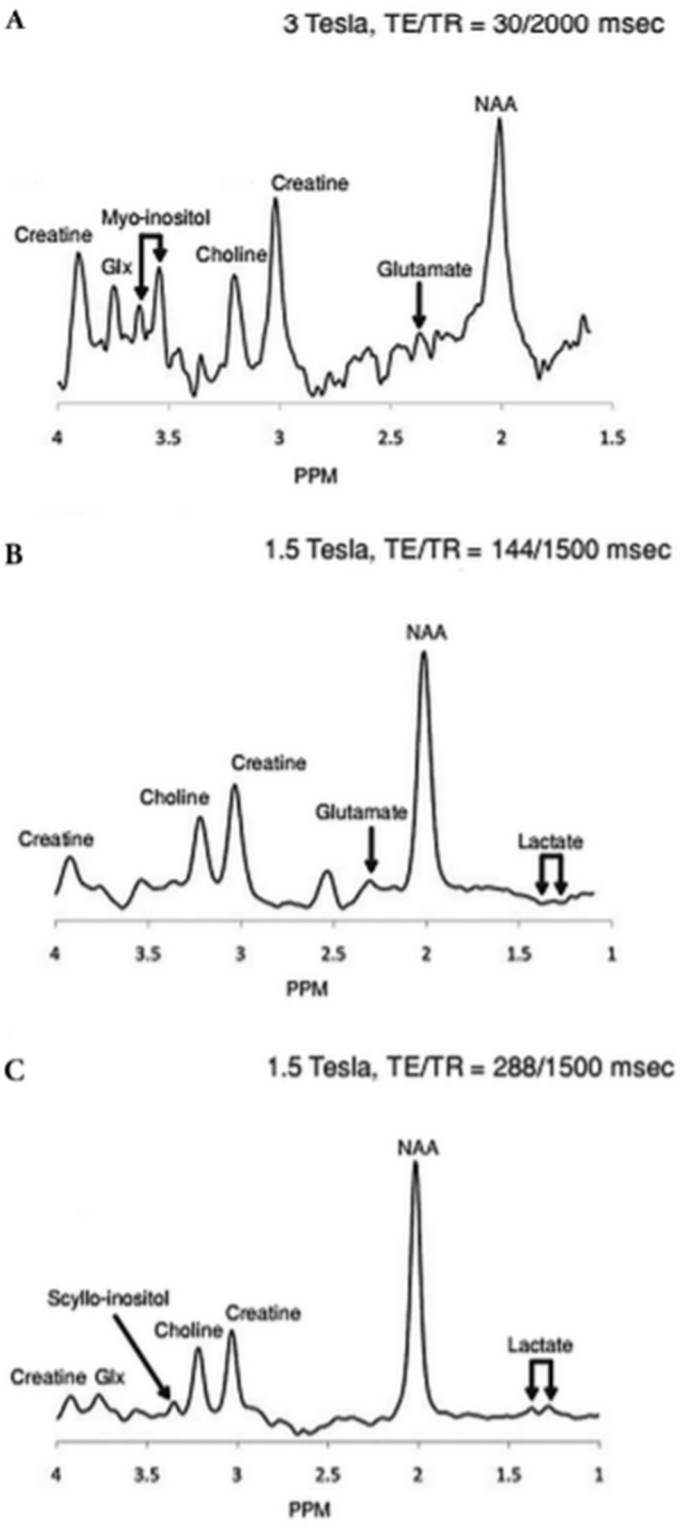

Fig 3. MRS spectrum in 3 different echo times

Normal brain metabolites

CHEMICAL COMPOUND	CHEMICAL SHIFT	COMMENTS
N-Acetylaspartate (NAA)	2.0	Neuronal marker.
Creatine/phosphocreatine	3.0,3.9	Energy metabolism. Supplier of phosphate to convert ADP to ATP.
Choline (cho)	3.2	Cell membrane marker.
Myo–inositol (ml)	3.6	Glial cell marker, osmolyte hormone receptor mechanisms
Glutamate (glu) Glutamine (Gln) (Glu+Gln=Glx)	2.1-2.5	An excitatory neuro transmitter and regulator
Lipids (lip)	0.9-1.4	Cell break down/ brain destruction indicator.
Lactate (Lac)	1.3	An end product of anaerobic glycolysis

Fig 4. Normal Brain metabolites

Metabolites in Spectroscopy spectrum:[17]

Lipids:

Lipids are peaks that are seen at 0.9 and 1.2 ppm. Lipid peak is not seen in the normal spectrum as the quantity of lipid is minimal in healthy tissues. The lipid peak is seen in tuberculous granulomas and brain tumors due to necrosis.

Lactate:

Lactate is seen as a doublet peak at 1.33 parts per million. MRS lactate is not detectable in healthy brain parenchyma. Lactate (Lac) is due to anaerobic glycolysis in cases like hypoxic brain tissue like stroke, encephalopathies, mitochondrial myopathies, lactic acidosis, cardiac dysfunction and neonatal hypoxic encephalopathies. It is used to diagnose necrotic cores in the brain tissue. It is seen in abscesses and cysts of different types. Lactate levels may be elevated secondary to inflammation as well.

Choline:

Choline/triethylamine (TMA) is a chemical in many water-soluble components of the brain tissue like myelin sheath and cell membrane. Resonation of the choline takes place at 3.2ppm. Pathological changes in membrane turnover (tumors, leukodystrophies, MS) resulting in significantly elevated choline peak. Choline is raised in active demyelinating lesions as phospholipids in the cell membranes are released during active myelin breakdown. Brain tumors associated with their high cellular density also show choline peak. MRS choline is physiologically elevated in infants.

Creatine:

Creatine (Cr) is a surrogate marker serving as an internal standard for comparison against other metabolites. The Cr peak resonates at 3.0ppm. It is the marker for intracellular ATP energy reserves in the neural tissue. Focal reduction in Cr peak is noted in the destructive pathologies like tumors. MR Spectroscopy permits the comparison with contralateral homologous regions in cases where the contralateral region is normal.

N-Acetylaspartate (NAA):

N-Acetylaspartate resonates at 2.0 parts per million (ppm). It is an AA derivative produced within the neurons and gets transported downhill in the axons. It is a very specific marker of viable neuroparenchyma. The most important role of NAA is to quantify the neuronal injury or loss in a predefined region. Neuronal integrity can also be assessed with help of NAA. The NAA/Cr ratio rises during the first few years after which they increase >1% a year until reaching the adult range by 16 years.

Pathologies like degenerative disorders, stroke and multiple sclerosis result in reduction in the NAA concentrations. Canavan's disease results in markedly elevated NAA levels.

Myoinositol:

Myo-inositol is a polyol (molecules similar to sugar) which resonates at 3.5 parts per million (ppm). Myo-inositol serves as an osmolyte for volume regulation in the brain. It is useful in the diseases that affect Choline levels. Since it is both glial marker and osmolyte, Myo-inositol levels can vary in cases of hepatic encephalopathy, dementia and hyponatremic brain syndromes.

Glutamine-glutamate-GABA complex (Glx):

It is constituted by chemically related amino acids(AA) and amines. They invoke the excitatory and inhibitory impulses. It resonates between 2.1 to 2.4 parts per million. As they are components of Kreb's cycle, it can potentially serve as an important marker(s) of stroke, lymphoma and various metabolic brain disorders.

Water and fat suppression:

Water and fat in the tissues are present in significantly increased concentration than the metabolites, which is why they produce signals which are many times the intensity as compared to that of metabolites. This results in difficulty in recording the relatively small signals from the metabolites. Hence, it is necessary to suppress the excessively large signals from fat and water.

Technique of suppression includes selectively saturating the water or fat resonance by inverting the magnetization of the water or fat and acquiring the spectrum study at a time when they have zero magnetization.

CNS INFECTIONS

Central nervous system (CNS) infections—i.e., infections involving brain parenchyma (cerebrum and cerebellum), spinal cord, optic nerve and the covering membranes—are infections that are associated with substantial morbidity, mortality, and long-term sequelae that can have catastrophic implications for the infected individuals.

Acute CNS infections fall broadly into three categories—meningitis, encephalitis, and abscesses.[18]

ETIOLOGY OF CNS INFECTIONS

A. BACTERIAL

- Pyogenic abscess
- Tuberculoma and tuberculous abscesses
- Mycobacterium avium- intracellulare infection
- Syphilis
- Listeriosis

B. FUNGAL

- Nocardiosis
- Actinomycosis
- Rhodo-coccosis
- Histoplasmosis
- Coccidioidomycosis
- Aspergillosis
- Mucormycosis
- Paracoccidioidomycosis
- Cryptococcosis

C. PARASITIC

- Neurocysticercosis
- Toxoplasmosis
- Amoebic brain abscess
- Echinococcosis
- Cerebral sparganosis
- Chaga's disease

DIFFERENTIAL DIAGNOSIS ACCORDING TO THE SIZE OF THE LESIONS

A. MILIARY

- Metastasis
- Tuberculoma

B. SMALL

- Metastasis
- Tuberculoma
- Cysticercus granuloma
- Inflammatory disorders of brain (vasculitis, Behcet's disease)
- Sarcoidosis

C. MEDIUM

- Sarcoidosis
- Metastasis
- Primary brain tumor
- Fungal granuloma
- Tuberculoma
- Toxoplasmosis

D. LARGE

- Cerebral abscesses
- Tuberculous abscesses
- Primary brain tumors
- Fungal abscesses
- Tumefactive demyelinating lesions

ENCEPHALITIS

Encephalitis is diffuse infection of the brain parenchyma. Infectious encephalitis is generally of viral etiology. Various non-viral causes of encephalitis are bacteria, fungus, parasites, and rickettsial organisms. The two types of encephalitis are primary & secondary encephalitis. Primary encephalitis occurs if there is direct involvement of the neuroparenchyma by the virus. If there is spread of infection from another part of the body it is termed as secondary encephalitis.[19]

HERPES ENCEPHALITIS (HSE)

It is of two types: neonatal and adult type. In adult type, the causative agent is Type I herpes simplex virus and it generally affects the frontal and temporal lobes. Type II Herpes virus causes neonatal encephalitis and results in diffuse brain involvement. MR imaging shows T2 hyperintensities in both the cortex and the subcortical brain matter of temporal lobe, frontal lobe, insular cortex bilaterally with involvement of cingulate gyrus occasionally. The lesion can show restricted diffusion, gyral edema with mild or no enhancement.[20]

HIV ENCEPHALITIS

Human immunodeficiency virus (HIV) acts by binding to the CD-4+ receptor located in the Langerhans cell, which progressively kills the CD-4+ T-cell which leads to release of a large viral load resulting in generalized dissemination in the body. The HIV-infected cells can cross the blood-brain barrier. Common features on MRI include volume loss of the brain parenchyma with reduction in cortical gray/white matter volume. Bilateral patchy symmetrical hyperintensities are seen on T2W images / FLAIR sequences involving the white matter without causing any mass effect. These patchy lesions do not show

enhancement or show diffusion restriction. MRS shows reduced NAA levels with raised choline and myo-inositol.[21]

The main differential diagnoses is progressive multifocal leukoencephalopathy (PML) and is caused by John Cunningham (JC) virus. It is an opportunistic infection and shows multiple focal lesions with involvement of the white matter in the posterior fossa which are asymmetrical. Solitary lesion tends to be seen in the subcortical 'U' white matter.

Proton-MRS shows decreased NAA, elevated choline, increased lactate and lipids. In a few cases increased myo-inositol levels can be seen. MTR imaging plays a helpful role in differentiation between HIV encephalopathy and PML.[22]

JAPANESE ENCEPHALITIS

This is a common disease in the South-Asian population and is transmitted by bite of the Culex mosquitoes. JE has a high rate of fatality with chances of post infectious sequelae in the survivors. T2 and FLAIR hyperintensities are seen in bilateral thalamus and brainstem. Unilateral lesions are far less common. There is a possibility that lesional hemorrhage may occur, which will be seen as patchy areas of blooming on GRE sequences. The lesions do not show enhancement on contrast injection.

DENGUE ENCEPHALITIS

Dengue encephalitis can occur due to severe infections by the dengue virus. MRI shows T2 hyperintensities in bilateral thalami and globus pallidi. Bilateral hippocampus, temporal lobes and brainstem are common sites of involvement. The lesions can show restricted diffusion with variable enhancement on contrast injection.

VARICELLA ZOSTER ENCEPHALITIS (VZE)

Varicella-zoster encephalitis can affect both adults and children. Neurological symptoms generally appear ten days after the initial chickenpox rash or post varicella vaccine. VZE more frequently presents as meningitis (>50%) than encephalitis (40%).

VZE presents as cerebellitis, myelitis with hyperintensities on T2WI sequence which usually restrict on diffusion-weighted sequence (DWI). Intralesional bleeds may be present in the form of areas of blooming on the GRE sequence with patchy enhancement in VZE. MRS shows raised choline (Cho) levels and reduced N-acetyl aspartate (NAA) levels.

Other rarer causes of viral encephalitis are rabies, cytomegalovirus, Creutzfeldt-Jakob disease and West Nile virus.

CEREBRITIS AND ABSCESS

Cerebritis is an ill-defined inflammation due to infectious etiology. Cerebritis can be due to different etiological factors, which include pyogenic infection, and if allowed to progress leads to abscess formation in the brain.

A pyogenic abscess is a focal brain infection. It is characterized by an area of pus in the center which is surrounded by a capsule. Brain abscess can be single or multiple. Brain abscess are often due to hematogenous spread of bacteria from another primary infection. Direct spread of the organisms occurs in cases of otomastoiditis, sinusitis, and odontogenic abscesses. Immunodeficiency is a major risk factor for developing pyogenic brain abscesses in conditions like HIV infection, post organ transplant patients, IV drug abusers, immunochemotherapy and diabetes.

STAGES OF ABSCESS FORMATION[24]

EARLY (3-5 DAYS) AND LATE (5-14 DAYS) CEREBRITIS STAGE

Early cerebritis is the stage of initial infection of brain parenchyma and is characterized by edema, vascular congestion and patchy coagulative necrosis. T1W images may show cerebritis as ill-defined, isointense to hypointense area relative to adjacent normal brain parenchyma, On FLAIR and T2WI focal areas of hyperintensities are seen which show patchy restricted diffusion. Late cerebritis is characterized by progressive infection and shows ill-defined increased hyperintensities on T2 and FLAIR imaging that shows progressive diffusion restriction and peripheral enhancement.

EARLY (2-4 WEEKS) AND LATE(WEEKS TO MONTHS) CAPSULE STAGE

They are differentiated on the basis of perilesional edema which is present only in the early stage of capsule formation. On T1WI, the lesion shows central hyperintensity. The rim is isointense on T1WI and hypointense on T2WI. The abscess ring is generally smooth, regular in thickness, and thin walled (approximately 5.0 mm thickness) which is its sine qua non.

Brain abscess tend to demonstrate high signal intensity on DWI sequence, which reverts on the ADC sequences. This is in direct correlation with the cellularity of the viscous pus within an abscess cavity.

The MR spectroscopy (MRS) values derived from the central necrotic area of abscess are fairly characteristic. In an untreated abscess, different resonating peaks may be seen corresponding to acetate at 1.92 parts per million(ppm), lactate at 1.3 parts per million(ppm), alanine at 1.5 parts per million(ppm), succinate at 2.4 parts per million(ppm) and pyruvate, as well as a complex peak at 0.9 parts per million(ppm) indicating amino

acids(AA) (valine, leucine, and isoleucine). They are the metabolic end products arising from aerobic and anaerobic respiration in the offending microorganisms.

Metabolites like succinate, alanine, acetate, isoleucine, leucine and valine are specific metabolites present in the pyogenic abscesses. However cysts due to parasitic origin show succinate and acetate without amino acid (AA).[5]

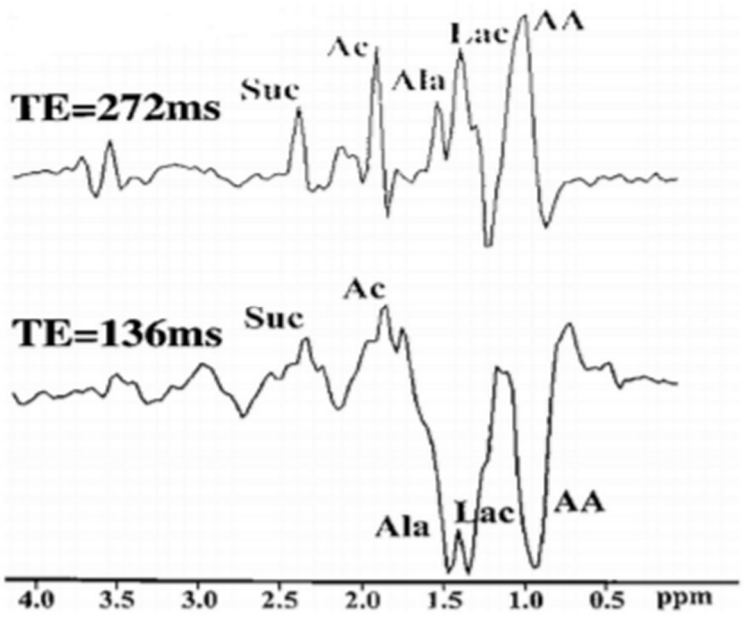

Fig 5 : Variable TE with variation in the amino acid and alanine levels

TUBERCULOMA

CNS tuberculosis can have a variety of presentations which include tubercular meningitis, tubercular abscess, focal cerebritis and tuberculomas. Tuberculomas can be found anywhere within the brain and can vary in number from single or multiple. The size of the lesions may vary from 1.0 mm to 8.0 cm. Tuberculomas originate as microgranuloma in the region of tuberculous cerebritis with further coalescence to form granuloma. This is followed by central solid caseous necrosis which might liquify in later stages.

Tuberculoma appearance can vary on MRI scans according to its stage. A non caseating tuberculoma usually shows hyperintense signals on T2WI and hypointense signals on T1WI. A solid tuberculoma appears iso to hypointense on T1WI and T2WI with T2 hyperintense rim and rim enhancement. If perilesional edema is present, it is difficult to distinguish the rim separately on T2WI. However, the central necrotic areas start to appear T2W hypointense rim on T2 and rim enhancement on post contrast study as liquefaction progresses.

MRI findings of tuberculomas commonly overlap with other infectious lesions, like that of NCC, brain abscesses and fungal granulomas. Few cancers and metastases appear similar to tuberculomas.

In vivo MR spectroscopy shows only lipid within the tuberculomas, at 0.9 and 1.3 ppm while a tuberculoma showing heterogeneous appearance can show choline peak at 3.22 ppm along with lipid. Lipid resonances at 0.9 and 1.3 parts per million(ppm) and is present at the center of a tuberculoma. The cell structure of a mycobacterium bacillus is known to contain lipids as saturated fatty acids as they are involved in the production of tubercle. According to a study by Ravishankar P M et al 94% of tuberculomas show a lipid peak in the range of 0.9 to 1.3 ppm.[25]

In addition to these findings lactate peak and elevated choline might be also present.

NEUROCYSTICERCOSIS

It is one of the most prevalent parasitic CNS infections in Asian countries. The tapeworm, Taenia solium, found in uncooked pork is an infectious organism. Each cyst measures approximately 3.0-18.0 mm and contains a scolex within it. If the cyst is alive, it can provoke a mild perilesional inflammation. It can remain viable for a period of

approximately 2-6 years after infection. The cyst induces an inflammatory reaction in the adjacent neuroparenchyma with edema and mass effect as it dies due to leakage of antigenic metabolic products. The patient then shows symptomatic seizures or focal neurological defects. The clear cyst fluid changes its color and shows turbidity and gelatinous. The degenerated cyst then collapses and often calcifies.

The cyst is commonly found in locations like basal meninges, intraparenchymal, intraventricular or the combination of the above mentioned sites. Intraparenchymal cysticercosis has been classified into the following 4 stages.

1. **Vesicular Stage**

After the implantation in the brain, the larva develops into a cyst containing the scolex. In approximately 3-12 months, the cysticercus reaches its adult size and shows clear fluid in the cyst. Mature cysts are visible on CT/ MRI scans and measure 5-20 mm. Cysts are commonly located at the gray-white matter junction and can also be present in bilateral basal ganglia, cerebellum and the brainstem. The cyst is typically thin and shows smooth walls, and a scolex is identified attached to the cyst. There is minimal to mild perilesional edema at this stage.

CT demonstrates a nonenhancing/mildly enhancing cyst wall containing a scolex and hypodense cystic fluid. A low-signal-intensity cyst cavity containing an isointense or hyperintense nodule can be seen on T1WI MR. On T2W MRI scan the scolex demonstrates isointensity, however it might be obscured by high T2 signal intensity fluid.

2. Colloidal Vesicular Stage:

The degeneration of the larva begins in this stage. The host's inflammatory response activates and results in formation of a fibrous capsule with surrounding perilesional edema. Diffuse encephalitis may occur after administration of the oral anthelmintic drugs.

CECT demonstrates cystic ring-enhancing lesions with hyperdense content and prominent perilesional edema. T1WI shows a hyperintense cyst owing to the proteinaceous dominant content in the cyst. T2WI shows a hyperintense cyst with perilesional edema.

3. Granular Nodular Stage

The cyst retracts and forms a nodule which later calcifies. CECT demonstrates an enhancing lesion with perilesional edema. MR images demonstrate a thick walled enhancing ring or nodule with/without perilesional edema, This appearance can simulate a tuberculoma, granuloma, or metastasis.

4. Nodular Calcified Stage

The lesion shrinks significantly and shows calcification. It appears as single or multiple calcified lesions on CT. As they are calcified, these nodules are hypointense on all MR sequences.

Cisternal Cysticercosis

Cisternal and spinal cysticercosis are quite rare and are frequently associated with parenchymal cysticercosis with primary involvement of subarachnoid spaces. Cysts may cause obstructive hydrocephalus due to mass effect or basilar arachnoiditis. The cysts in the subarachnoid spaces generally lack a scolex.

Intraventricular Cysticercosis

It is characterized by the intraventricular location of the cysts. The serious complications include obstructive hydrocephalus and ventriculitis. On MR images, the scolex, subependymal inflammation and cyst wall are easily visible within the ventricles.[26]

On MRS of cysticercosis- raised levels of alanine, lactate, succinate and choline (Cho) with decreased levels of creatine and NAA.

Vasudev MK, Jayakumar PN. Srikanth SG. Nagarajan K. Mohanty A (2007) studied 33 patients using T2WI and T1WI (with and without Magnetization transfer) and DWI sequences correlating them with the ADC values. They came to a conclusion that CNS tuberculoma showed shorter T2 relaxation time, reduced MTR, and no evidence of diffusion restriction. Lipids as marker for tuberculoma were first suggested by Gupta RK et al. [27,28]

Kallita J, Prasad D, Maurya DS, Kumar SD (2012) did a study on 67 patients with TB meningitis underwent MRI and MRA evaluation. They concluded that 50% of the TB meningitis patients showed abnormal MR angiography involving posterior and anterior circulations and 62% of the patients had brain infarcts.[29]

Batra A. Tripathi RP (2004) studied 16 patients with single or multiple lesions. DWI sequence was done with b' values of 50, 600, and 1100 s/mm2 and the ADC maps were calculated. MR spectroscopy was performed using the SV technique with two medium and long echo times 130 ms and 280 ms. They came to a conclusion that DWI and MR spectroscopy can help in diagnosis of the CNS tubercular lesions; however, they don't assist in specific characterisation.[30]

Gupta RK, Husain M. Vatsal DK. Kumar R. Chawla S, Husain N. (2002) have analyzed the values of in-vivo H+ MRS and TIW MT imaging in tissue characterization of brain tuberculomas in 33 patients of proven CNS tuberculoma with Proton MRS and T1W MT MR imaging and they came a conclusion that T1W MT MRI is better for the characterization of CNS tuberculoma.[31]

Salgado P, Del Brutto OH, Talamás O. Zenteno MA, Rodríguez Carbajal J. (2005) reviewed MR studies of 6 patients with intracranial tuberculoma. CT and MR, show equal sensitivity in diagnosis of the CNS tuberculoma, MRI was better to demonstrate the extent of lesions. However, the potential role for MR diagnosis of intracranial tuberculoma is limited by the fact that other infectious or neoplastic diseases may present similar findings.[32]

Chang KH, Han MH, Roh JK, Kim 10, Han MC, Choi KỲ, Kim CW (1990) reviewed twenty-six patients with intracranial tuberculosis (Tb) (10 with acute meningitis, 5 with chronic meningitis, 5 with meningitic sequelae and 6 with localized tuberculoma(s) were examined with MR before and after Gad-DTPA enhancement. MR imaging appears to be superior to CT in evaluation of active intracranial Tb only if Gad-DTPA is used, while CT is better than MR in evaluating meningitic sequelae with calcification.[33]

Amaral L, Maschietto M. Maschietto R. Cury R. Ferreira NF, Mendonça R. Lima SS (2003) retrospectively analysed 172 cases of neurocysticercosis in MR studies carried out over a period of 13 years. They concluded that MR imaging is a sensitive and specific method in the analysis of different forms of unusual manifestations of neurocysticercosis. which should appear in the differential diagnosis of parenchymal, ventricular, spinal, cisternal, and orbital lesions.[34]

Chang KH, Han MH reviewed MRI findings of parasitic disease of the central nervous system (CNS) in 1998, with emphasis on neurocysticercosis which is by far the most common CNS parasitic infection worldwide. They concluded that MRI is superior to CT in the evaluation of most CNS parasitic infections and is nearly diagnostic, particularly in endemic areas. Contrast enhanced studies is essential not only for specific diagnosis of the disease, but also for the assessment of the inflammatory activity.[35]

HR Martinez R Rangel- Guerra, G Elizondo, J Gonzalez, LE Todd, J Ancer, and SS Prakash reviewed the MR findings in 56 patients with neurocysticercosis (NCC) in 1989, MR finding were correlated with other neuroradiological finding in 40 cases with histopathological studies in 15 surgically treated patients, and with autopsy finding in one case. They concluded that MR is sensitive in diagnosing active NCC and may be useful in evaluating the degenerative changes in parasite that occur as a result of natural degeneration, host response or medical therapy.[36]

Savita R Singhal, Smiti Nanda and Suresh K Singhal report the cases of two Indian women, aged 20 and 24 years old respectively, with neurocysticercosis presenting in the second trimester of pregnancy with convulsions. Neurocysticercosis should be considered in pregnant women presenting with seizures which cannot be explained by eclampsia, especially in early pregnancy.[37]

D. Pal, A. Bhattacharyya,M. Husain, K.N. Prasad, C.M. Pandey, R.K. Gupta evaluated Conventional MR imaging and in vivo IH-MR spectroscopy data from 194 patients with pyogenic brain abscesses, with ages ranging from 3 to 60 years. They concluded that the presence of AAs on in vivo IH-MR spectroscopy is a sensitive marker of pyogenic abscess, but its absence does not rule out a pyogenic etiology. The presence of Ac with or without

Suc favors an anaerobic bacterial origin of the abscess; however, this may also be seen in some of the abscesses secondary to facultative anaerobes. [38]

Mao J. Li J. Chen D, Zhang J. DU YN, Wang YJ. Li X, Wang R., Chen LY, Wang XM (2011) retrospectively studied The clinical data of 8 premature infants with central nervous system invasive fungal infection (IFI). They concluded MRI-DWI and serial MRIs are helpful in the early diagnosis of candida cerebral abscess and the evaluation of treatment outcome in premature infants.[39]

G. Luthra, A. Parihar, K. Nath,S. Jaiswal,K.N. Prasad et al (2007) performed a retrospective analysis on 110 patients with surgically proved brain abscesses. Imaging studies included T2, T1 post contrast T1, DWI, and PMRS. They concluded that based on the morphologic, ADC, and metabolite information, it may be possible to differentiate among the pyogenic, tubercular, and fungal brain abscesses.[40]

Kazuhiro Tsuchiya, Sayuki Inaoka, Yoshiyuki Mizutani, and Junichi Hachiya compared fast FLAIR images with conventional spin-echo images (TI and T2-weighted) obtained in 20 patients with infectious diseases. They concluded that Fast FLAIR images showed pathologic changes in intracranial infectious diseases better than or as well as conventional T2- and proton density-weighted spin-echo sequences. However, postcontrast T1-weighted spin echo sequences resulted in better visibility of abscess, meningitis, cysticercosis, and epidural empyema than did FLAIR images.[41]

Shukla-Dave A, Gupta RK, Roy R, Husain N, Paul L, Venkatesh SK, Rashid MR, Chhabra DK, Husain M (2001) evaluated fifty-one patients with intracranial cystic lesions (21 abscesses, 20 gliomas, 3 hydatid cysts, 3 arachnoid cysts, 1 case each of glioependymal cyst, xanthogranuloma, infarction and acoustic neuroma) were evaluated with conventional MR imaging and in vivo PMRS.. In vivo PMRS accurately predicted the

pathology in 92% of the MR spectroscopy cases. We conclude that in-vivo PMRS complements characterization of cystic intracranial mass lesions.[42]

Kee-Hyun Chang. In Chan Song, Sung Hyun Kim, Moon Hee Han et al (1998) evaluated 40 proton MR spectra obtained from cystic contents of various intracranial cystic masses in 39 patients. They concluded that only lactate is commonly observed in a variety of intracranial cystic masses, except for abscess and cysticercosis, in which resonances of acetate, succinate, amino acids and/or unassigned metabolites can be seen in addition to a lactate peak.[43]

Gupta RK, Prakash M. Mishra AM, et al performed DWI in seventy tuberculomas and tuberculous abscesses in 30 patients were categorized in three groups depending on the intensity in the core of the lesion on T2 weighted images. They concluded that addition of DWI to routine imaging protocol may help in differentiation of tuberculous lesions from degenerating cysticercus granuloma.

R K Gupta 1, D K Vatsal, N Husain, S Chawla, K N Prasad, R Roy, R Kumar, D Jha, M Husain performed a study on 27 patients with brain abscesses and tuberculomas. They came to a conclusion that it is possible to differentiate tuberculous abscesses from pyogenic abscesses by using MT MR imaging and in vivo MR spectroscopy.[44]

MATERIALS AND METHODS

Source of data:

Patients who were referred for CT or MRI to the Department of Radio-Diagnosis at the KLE's Dr. Prabhakar Kore Hospital & MRC, Belagavi.

Method of collection of data:

Study design: Hospital based prospective observational study.

Sample size: Incidence and Prevalence of CNS infections varies with age and etiology in the Indian Population. Therefore, all cases with infectious brain lesions evaluated on magnetic resonance imaging during the study period will be the sample size.

Sampling method: Universal sampling

The minimum sample size formula based on prevalence is

$$n = \frac{z_\alpha{}^2 P(1-P)}{d^2}$$

where P is the percentage of prevalence and d is the percentage likely difference in the prevalence.

z_α is linked with the level of significance. For 5% level of significance $z_\alpha = 1.96$.

Ref:[45]

With P = 60.4% and d = 15% of P = 9.1%, the sample size is 48.

DURATION: January 1st 2020 to December 31st 2020.

Inclusion criteria:

1. Patients of CNS infections suspected clinically or detected by CT/MRI brain scan or lumbar puncture.
2. Patients who give consent to take part in the study.

Exclusion criteria:

1. Patients with known contraindications to MRI. (Hip implants, vascular clips)
2. Patients who are known case of CNS tumors or hemorrhage

Discrete variables will be represented by the median. Suitable graphs will be used to depict the comparison.

The categorical data will be expressed in terms of rates, ratios and percentages. The association between the outcome, clinical and demographic characteristics will be tested using Chi-square test, test of proportion or Fisher's exact test.

When we compare two independent groups having quantitative values, generally the student's unpaired t test is applied. For discrete variables nonparametric tests will be used.

For all the tests the value of p less than 5% (0.05) will be considered significant.

Methodology:

The subjects will be enrolled in the study after they give written informed consent for MRI spectroscopy of brain

A detailed history will be taken in the form of a systematic proforma regarding patient age, sex, past medical/surgical history.

After considering the inclusion and exclusion criteria, the patients will be taken up for routine MRI with spectroscopy of the brain. MRI brain of all the patients will be done using 3.0 Tesla MRI scanner (Magnetom Spectra, 32 channel; Siemens, Erlangen, Germany). Routine brain MRI will include conventional spin echo sequences like axial

FLAIR, DWI, ADC, SWI, axial & coronal T2 and axial & sagittal T1 sequences. Multi-voxel spectroscopy will be performed at TE 30/135 and voxels will be placed over the lesion as well as normal brain parenchyma. We used STEAM and T1 post contrast sequences as localization sequences with 5 mm thickness. Spectroscopy will be avoided in lesions close to the bone. Special sequences including CISS 3D or MPRAGE sequence will be used if required.

RESULTS

Table 1: Age wise distribution of cases

Age groups	Number of cases	% of cases
<=20yrs	4	8.33
21-30yrs	8	16.67
31-40yrs	6	12.50
41-50yrs	11	22.92
51-60yrs	13	27.08
>=61yrs	6	12.50
Total	48	100.00
Mean±SD	44.29±14.71 years	

Graph 1: Age wise distribution of cases

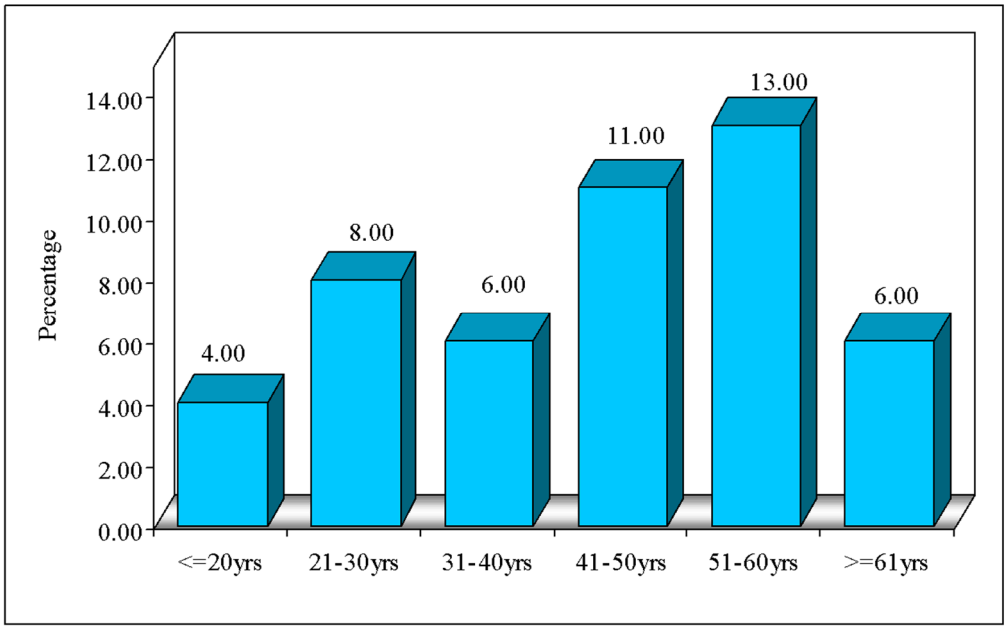

Table 2 : Gender wise distribution of cases

Gender	Number of cases	% of cases
Male	27	56.25
Female	21	43.75
Total	48	100.00

Graph 2: Gender wise distribution of cases

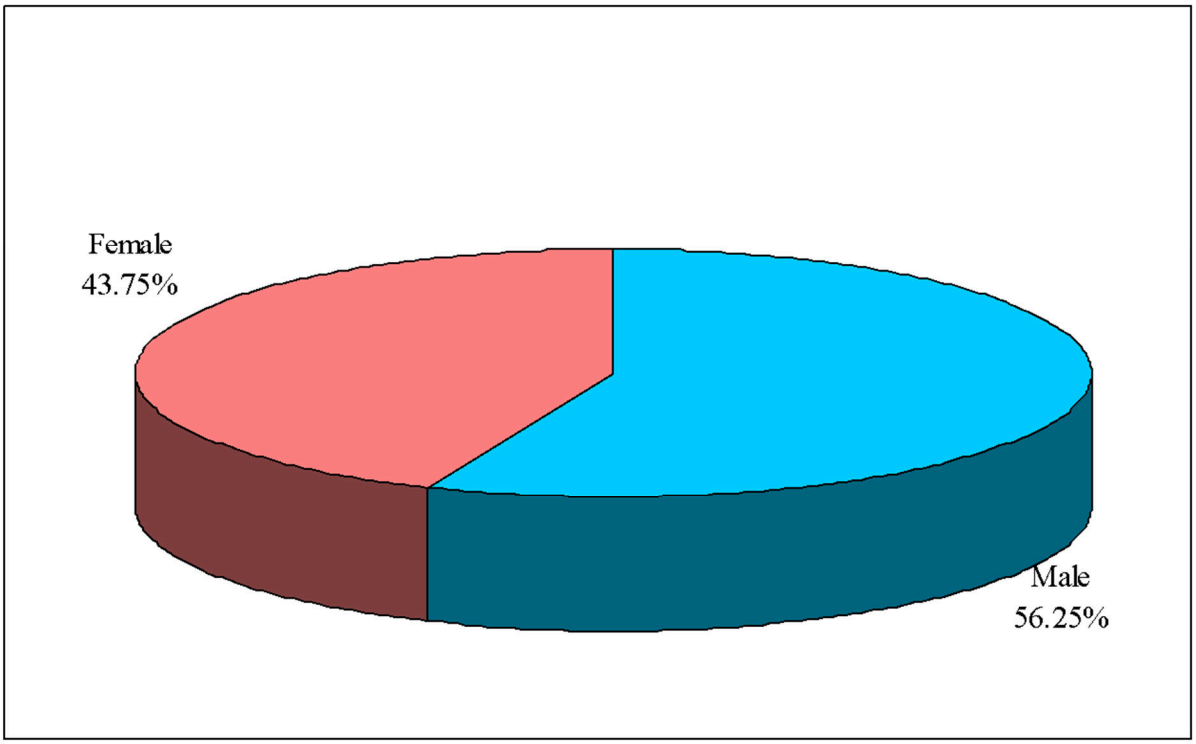

Table 3: Symptoms wise distribution of cases

Symptoms	Number of cases	% of cases
Altered sensorium	9	18.750
Ataxia	10	20.833
Fever	41	85.417
Headache	36	75.000
Motor weakness	5	10.417
Nasal blockage with discharge	1	2.083
Seizures	12	25.000
Vesicular rashes	1	2.083
Vomiting	35	72.917
Weight loss	1	2.083

Graph 3: Symptoms wise distribution of cases

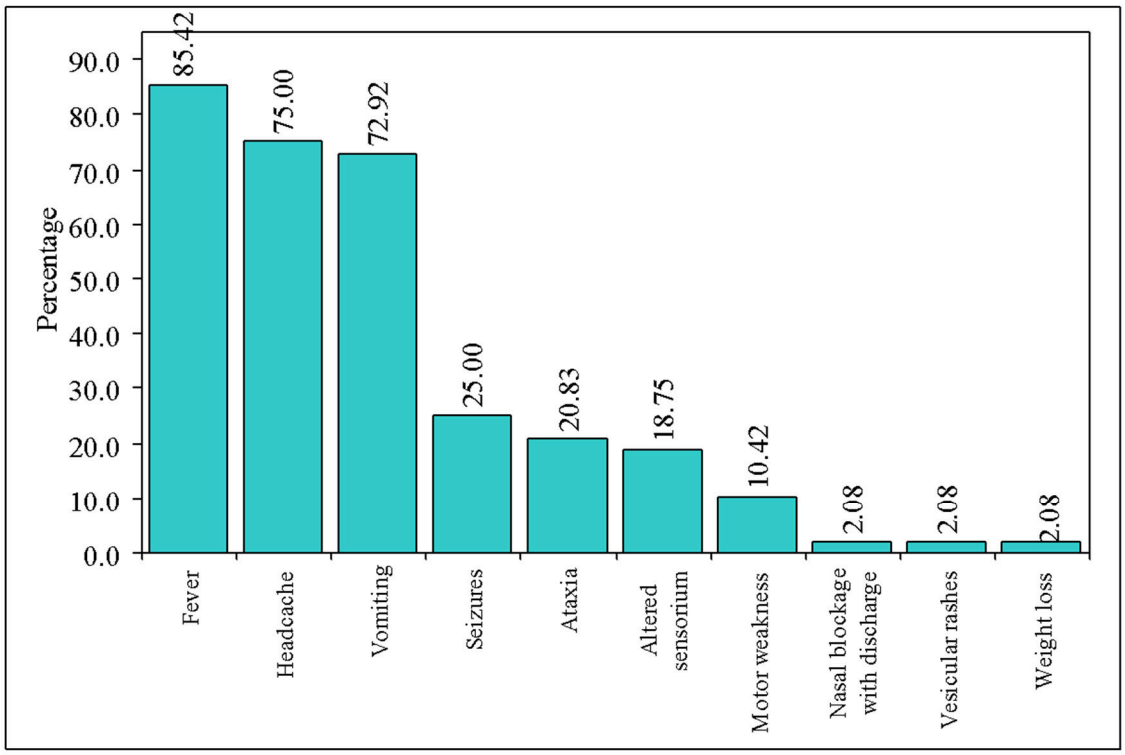

Table 4: Anatomical distribution of cases

Side of pathology	Number of cases	% of cases
Left side	15	31.25
Right side	6	12.50
Bilateral	27	56.25
Total	48	100.00

Graph 4 : Anatomical distribution of cases

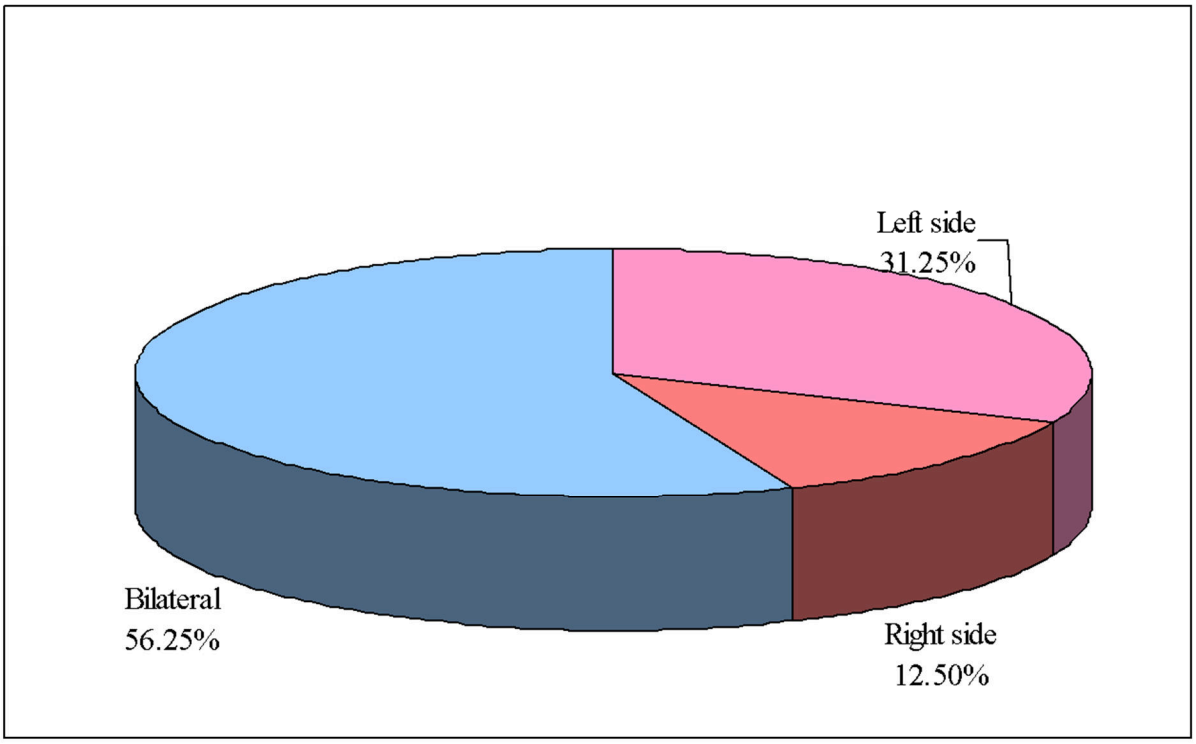

Table 5 : Number of lesions per case

Number of lesions	Number of cases	% of cases
1	12	25.00
2-4	8	16.67
>5	28	58.33
Total	48	100.00

Graph 5: Number of lesions per case

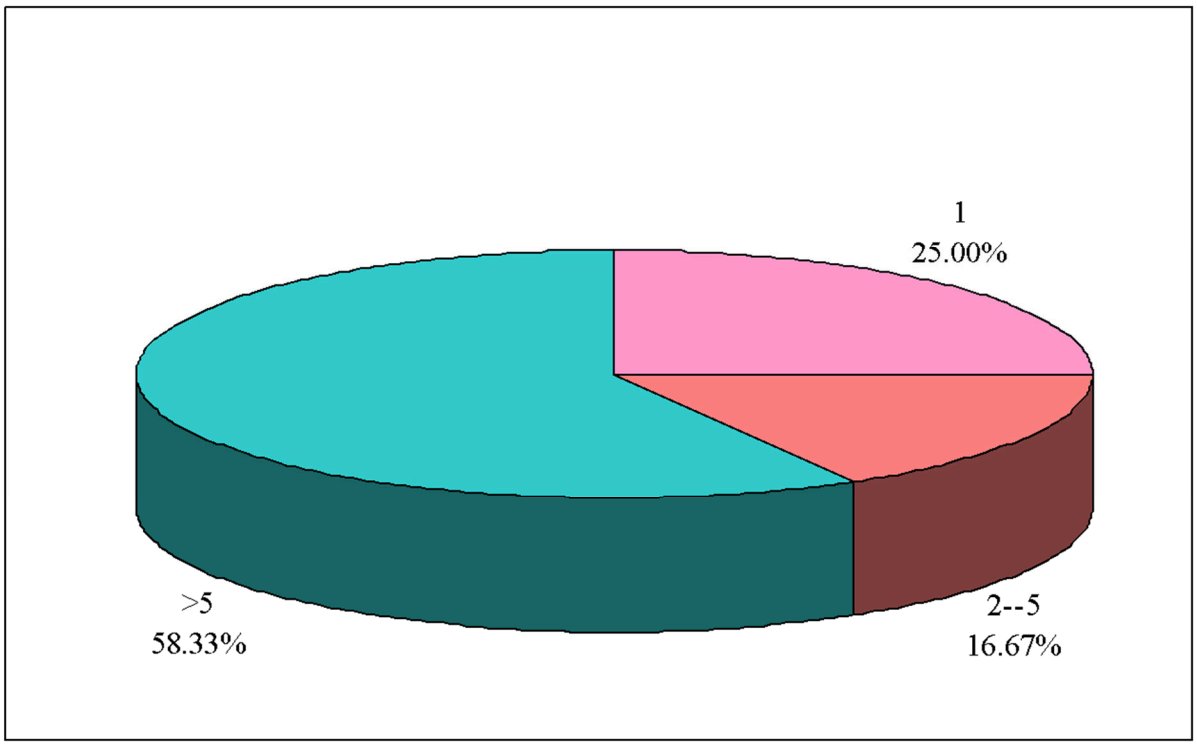

Table 6 : Morphological distribution of cases

Margins of lesions	Number of cases	% of cases
Ill-defined	14	29.17
Well-defined	34	70.83
Total	48	100.00

Graph 6: Morphological distribution of cases

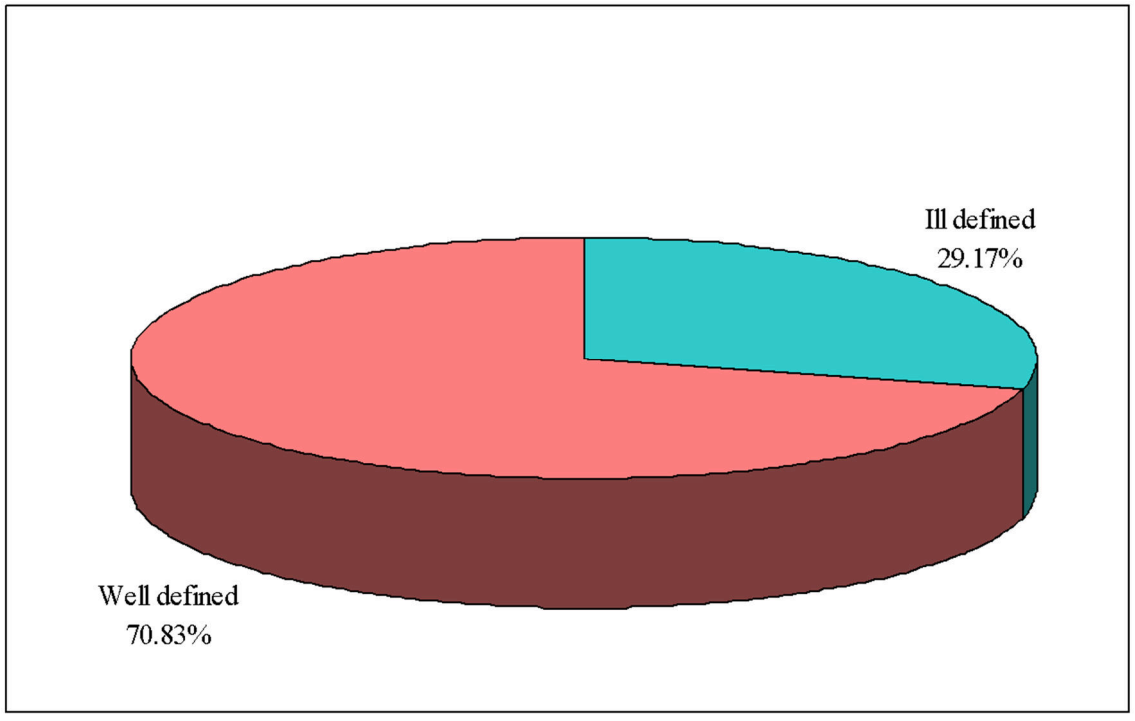

Table 7: Symmetry wise distribution

Symmetry	Number of cases	% of cases
No	41	85.42
Yes	7	14.58
Total	48	100.00

Graph 7: Symmetry wise distribution

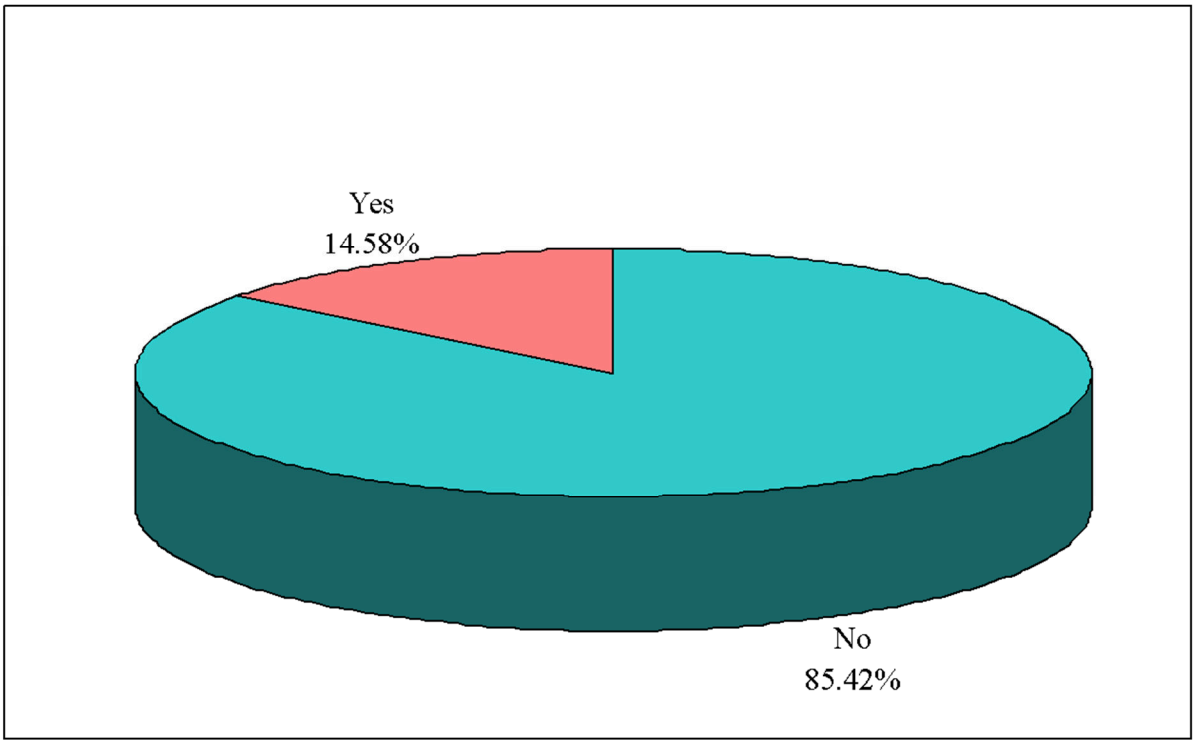

Table 8: Distribution of cases according to the T1 and T2 Morphology

Morphology	T1 morphology		T2 morphology	
	Number of cases	% of cases	Number of cases	% of cases
Hyperintense	3	6.25	31	64
Hypointense	1	39.58	9	18.75
Isointense	25	52.08	1	2.08
Mixed	0	0.00	2	4.17
Normal	1	2.08	1	2.08
Peripheral hypointense	0	0.00	4	8.4
Total	48	100.00	48	100.00

Graph 8: Distribution of cases according to the T1 and T2 Morphology

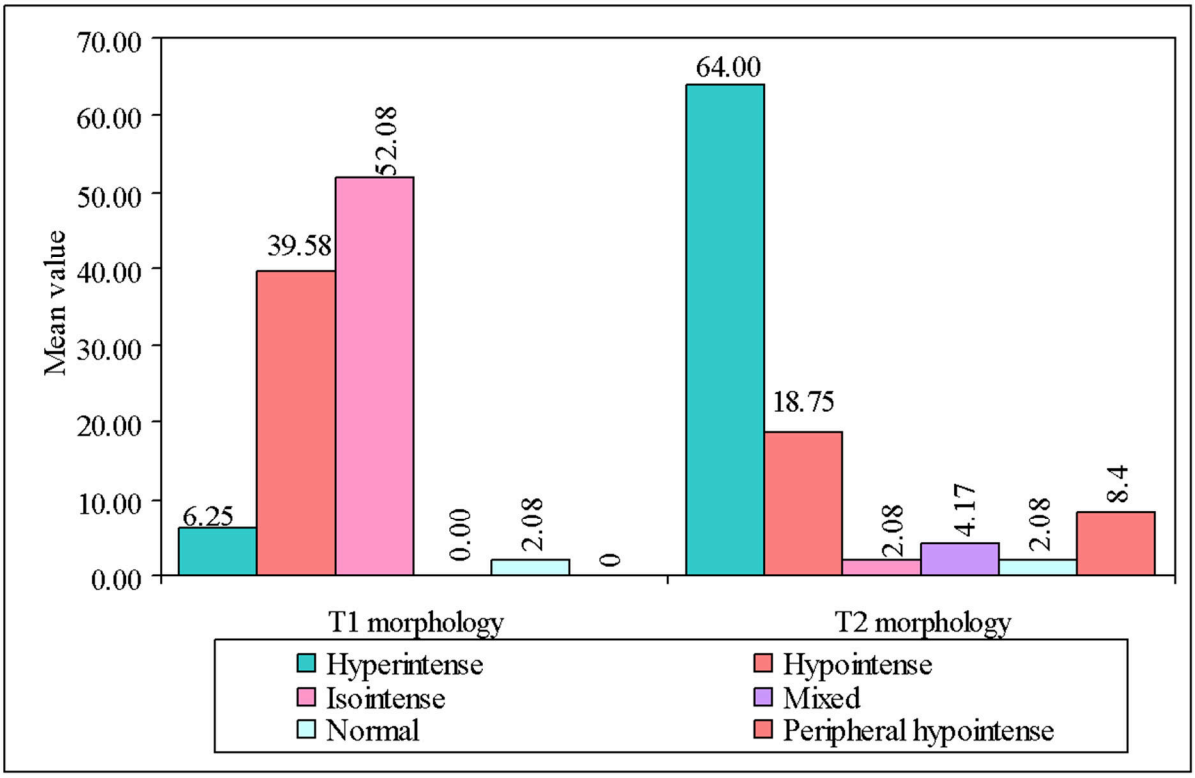

Table 9: Distribution of cases according to diffusion restriction

Diffusion restriction	Number of cases	% of cases
Absent restriction	20	41.67
Diffusion restriction	28	22.92
Central diffusion restriction	3	6.25
Peripheral diffusion restriction	13	27.08
Subtle restriction	1	2.08
Total	48	100.00

Table 9: Distribution of cases according to diffusion restriction

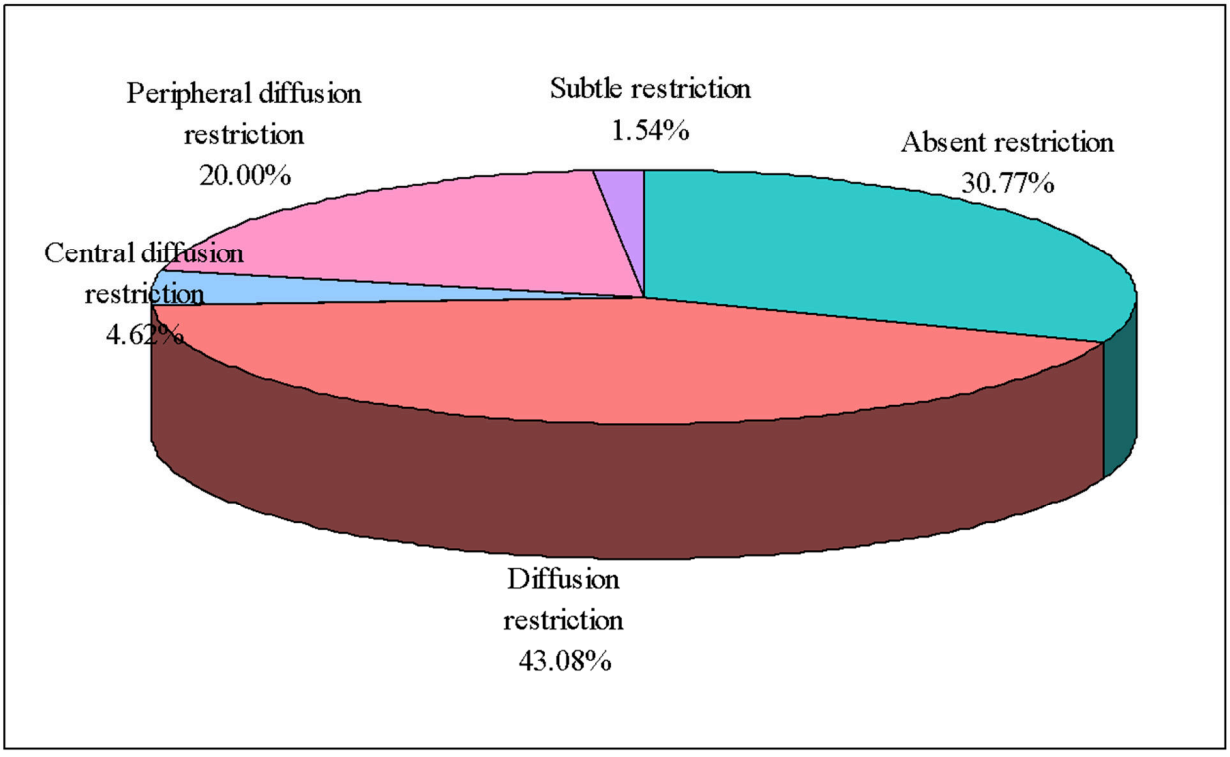

Table 10: Enhancement patterns

T1 C+ FS	Number of cases	% of cases
Non enhancing	2	4.17
Enhancement	32	68
Leptomeningeal enhancement	4	8.4
Ring enhancement	25	51.7
N/A	14	29.17

Graph 10: Enhancement patterns

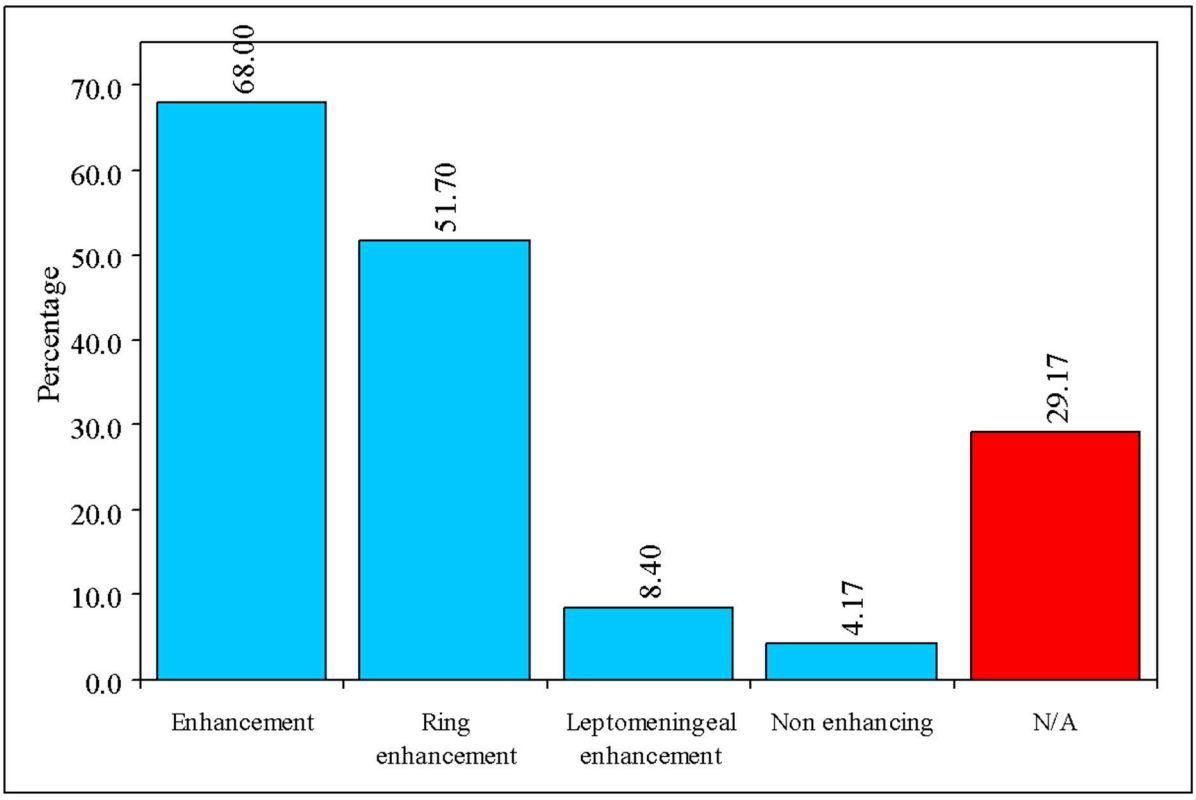

Table 11: Incidence of CNS infections

Radiological diagnosis findings	Number of cases	% of cases
Bacterial abscess	7	14.6
Cerebritis	2	4.1
Chronic tuberculosis	1	2.08
Cryptococcoma	1	2.08
Encephalitis (Cause uncertain)	3	6.25
Fungal abscess	3	6.25
HIV encephalitis	2	4.17
HSV encephalitis	5	10.42
Meningitis with ventriculitis	1	2.08
Meningoencephalitis	1	2.08
NCC	2	4.17
PML	4	8.33
Toxoplasmosis	6	12.50
Tubercular abscess	1	2.08
Tuberculoma	9	18.75
Total	48	100.00

Graph 11: Incidence of CNS infections

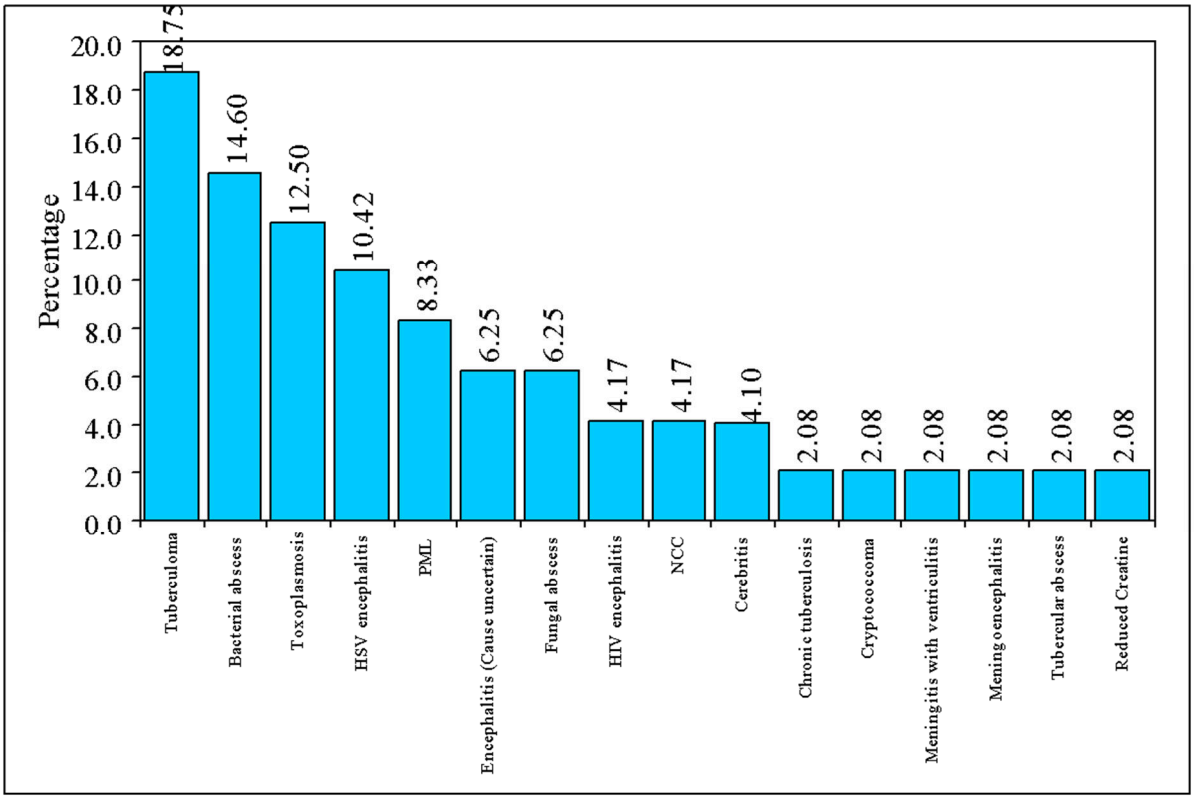

Table 12 : MR spectroscopy findings

MRS spectroscopy	Number of cases	% of cases
LL peak	25	52.08
Reduced NAA	16	33.33
Reduced NAA/Cr ratio	12	25.00
Increased Choline	5	10.42
Normal	5	10.42
Reduced Acetate	4	8.33
AA peak	3	6.25
Increased Ac/S ratio	3	6.25
Increased Lactate	3	6.25
Increased Alanine	2	4.17
Increased Cho/Cr ratio	2	4.17
Increased Trehalose	1	2.08
Increased Glx	1	2.08
Increased Glycine	1	2.08
Normal Ac/S ratio	1	2.08
Reduced Creatine	1	2.08

Graph 12: MR spectroscopy findings:

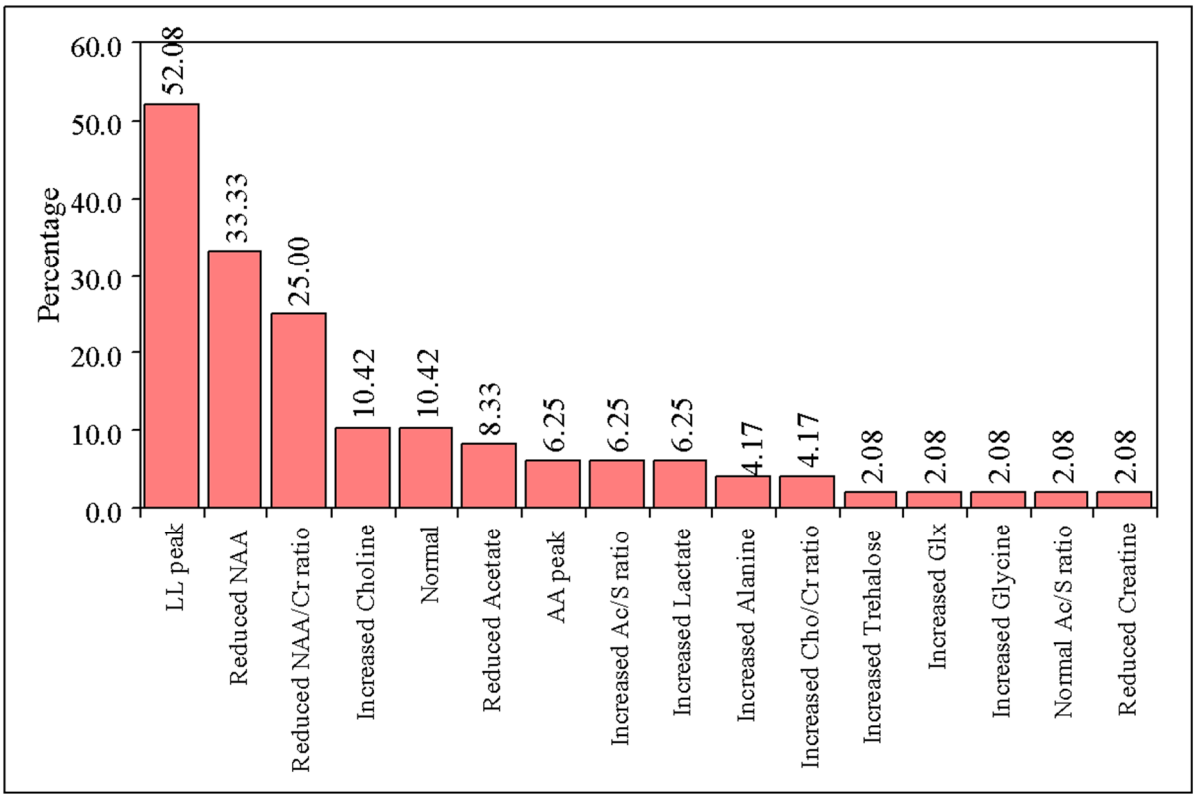

Table 13 : MR spectroscopy in CNS Infections

MRS spectroscopy	Bacterial abscess	Cerebral abscess	Cerebritis	Chronic tuberculosis	Cryptococcoma	Encephalitis	Fungal abscess	HIV encephalitis	HSV encephalitis	Meningitis with ventriculitis	Meningoencephalitis	NCC	PML	Toxoplasmosis	Tubercular abscess	Tuberculoma
AA peak	0	0	0	0	0	0	3	0	0	0	0	0	0	0	0	0
Increased Alanine	2	0	0	0	0	0	0	0	0	0	0	0	0	0	0	0
Increased A/S ratio	3	0	0	0	0	0	0	0	0	0	0	0	0	0	0	0
Increased Lactate	0	0	0	0	0	1	0	0	0	0	0	0	2	0	0	0
Increased Trehalose	0	0	0	0	1	0	0	0	0	0	0	0	0	0	0	0
Reduced NAA/Cr ratio	0	0	2	1	0	0	0	0	4	0	0	0	0	0	0	5
Increased Acetate	4	0	0	0	0	0	0	0	0	0	0	0	0	0	0	0
Increased Cho	0	0	0	0	0	0	0	0	0	0	0	0	4	1	0	0
Increased Glx	0	0	0	0	0	1	0	0	0	0	0	0	0	0	0	0
Increased Gly,	1	0	0	0	0	0	0	0	0	0	0	0	0	0	0	0
LL peak	6	1	0	0	0	0	0	0	0	0	0	0	2	6	1	9
Normal	0	0	0	0	0	2	0	0	1	1	1	0	0	0	0	0
normal A/S ratio	1	0	0	0	0	0	0	0	0	0	0	0	0	0	0	0
Reduced NAA	0	0	2	0	1	0	0	2	0	0	0	2	4	4	0	1
Reduced CR	0	0	0	0	1	0	0	0	0	0	0	0	0	0	0	0
Increased Cho/Cr ratio	0	0	0	0	0	0	0	0	2	0	0	0	0	0	0	0

DISCUSSION

Magnetic resonance imaging (MRI) is an excellent neuroimaging modality owing to its superior soft tissue contrast and multiplanar and noninvasive capabilities that can image the lesion accurately. MRI can provide an accurate assessment of the brain in CNS infectious lesions, accurate diagnosis, to begin immediate treatment and follow up.

This was a prospective study done in the Department of Radiodiagnosis and Imaging, KLES Prabhakar Kore hospital and MRC, Belagavi aimed at studying the MR appearances of various CNS infections of the brain and correlating the MR spectroscopy findings. In our study of MR imaging with spectroscopy was done for 48 patients with CNS infections. Brain MRI and MRS were assessed in patients with CNS infections and findings were compared. The diagnosis was confirmed by assessing response to therapy on follow-up examinations.

AGE-WISE DISTRIBUTION

Forty-eight patients were evaluated, whose age group ranged from 18 to 76 years. The CNS infections were most prevalent in the 51-60 years age group accounting for 27% of cases and the least prevalence was seen in the age group of 31-40 years constituting 12% with the mean age of the patients being 44 years.

SEX DISTRIBUTION

Our study included 48 patients, of which 21(43%) were females and the rest 27(56%) were males.

CLINICAL SYMPTOMS

Fever was the most common complaint by the patient in 85% cases followed by headache (75%) and vomiting (72%). Few patients presented with seizures(25%), ataxia(20%), altered sensorium(18%) and motor weakness(10%).

INFECTIONS

Among the 48 patients, tuberculosis (TB) was the most common etiology in 11(25%) of patients, out of which tuberculoma was the most common presentation in 9 (18%) patients. Encephalitis was the 2nd most common infection with 11 (22%) cases. Among the encephalitis, the most common etiology was HSV with 5 (10.5%) cases and 2 (4%) HIV cases. The diagnosis of 3 (6%) of encephalitis, presumed to be of a viral origin. Incidence of abscesses was 10 (20%) with 7 (14.5%) being of bacterial origin, 3 (6%) of fungal etiology and 1(2%) due to TB. Progressive multifocal leukoencephalopathy (PML) accounted for 4 (8%) cases while Neurocysticercosis (NCC) accounted for 2 (4%) of the cases. Meningitis and Cerebritis accounted for 2 (4%) cases each while cryptococcoma accounted for 1 (2%) case. Out of 48 patients 10 (21%) patients were immunocompromised due to HIV.

LESION MORPHOLOGY

Out of 48 patients who were studied, 27 (56%) patients had bilateral lesions while 15(31%) lesions were on the left side and 6 (12%) lesions were on the right side. 28 (58%) patients had five or more lesions. 8 (16%) patients had 2 to 4 lesions and 12 (25%) patients had a single lesion.

Among 48 patients, 34 (70%) patients had well-defined lesions as compared to 14 (30%) patients presenting with ill-defined lesions. Well-defined lesions were mostly attributed to

abscesses, tuberculomas and toxoplasmosis while ill-defined pathologies included meningitis and encephalitis. Only 7 (14%) patients with HIV encephalopathy and HSV encephalitis had symmetrical lesions.

CHARACTERISATION ON MRI

In our study, 20 (41%) lesions did not show any diffusion restriction while rest 28 (59%) showed diffusion restriction, out of which 13 (26%) showed peripheral diffusion restriction.

Out of 48 patients, 33 (68%) patients underwent contrast study out of which 25 (51%) cases showed ring enhancement, 4 (8%) cases showed leptomeningeal enhancement and 2 (4%) did not show any contrast enhancement.

TUBERCULOMAS

Out of forty-eight patients evaluated, tuberculomas were seen in 9 (19%) cases and 1(2%) case of tuberculous abscess. Among the 9 cases (5 male and 4 female), Single lesions were noted in 6 cases (27.2%) and multiple in 16 cases (72.7%). They generally appeared as T2 hyperintense lesions with few of them showing peripheral T2 hypointense halo. 4 out of the 9 lesions show peripheral diffusion restriction. On MRS, all the tuberculoma lesions showed a lipid lactate peak, with 4 lesions showing reduced NAA peaks. The tubercular abscess also showed lipid lactate peak within it.

CEREBRITIS & PYOGENIC ABSCESS

Out of 48 patients evaluated cerebritis was seen in 2 (4%) and pyogenic abscesses were seen in 7 (14%) of cases. Among the 9 cases 2 were females and the rest 7 were male patients. 4 patients presented with single lesion and 3 patients had multiple (>5) lesions.

On MRI cerebritis appeared as an ill-defined T2 hyper intense lesion with diffusion restriction, however all the abscesses appeared as a well-defined T2 hyperintense lesion with all of them showing ring enhancement. On MRS, both the cases of cerebritis showed reduced NAA with decreased NAA/Cr ratio. Among pyogenic abscesses 4 out of 7 cases showed an AA peak consisting of Acetate, Glycine and Alanine with 3 of the abscesses showing increased A/S ratio. 5(10%) of the abscesses also showed lactate peak at the centre.

D. Pal, A. Bhattacharyya, M. Husain, K.N. Prasad, C.M. Pandey and R.K. Gupta performed a study on 194 patients which showed resonance of AAs with or without other metabolites in 80% of abscesses.[46]

FUNGAL ABSCESSES

There were 3 cases of fungal abscesses in which 2 were associated with mucormycosis and 1 case had associated meningitis as well.

On MRS, all the abscesses showed Amino acid peaks with 2 of them showing Trehalose peaks at 3.6 to 3.8 ppm.

ENCEPHALITIS

Out of 48 cases, 11 (23%) patients presented with encephalitis in which 5(11%) had HSV encephalitis, 2(4%) had HIV encephalitis while 1 patient had meningoencephalitis. Etiology in 4 of the patients could not satisfactorily be determined.

On MRS, both cases of HIV encephalitis showed reduced NAA levels. 4 out of 5 cases of HSV encephalitis showed reduced NAA/Cr ratio while 2 of them also showed increased Ch/Cr ratio. 1 of the cases showed normal spectroscopy findings. Out of the 4 cases of encephalitis with uncertain etiology 3 cases showed normal findings on spectroscopy

while 1 showed Glx peak with increased lactate.[47]

TOXOPLASMOSIS

Out of 48 cases there were 6 (12%) cases of toxoplasmosis out of which 4 were males and 2 were female patients. All of the cases showed well-defined lesions in which 2 of them had single lesions and the remaining 4 patients had multiple lesions. 2 of the cases were associated with coexistent HIV infection.

On MRS, all the 6 patients showed lipid lactate peaks with 4 cases showing reduced NAA and 1 case showing increased choline.

PROGRESSIVE MULTIFOCAL LEUKOENCEPHALOPATHY

In our study 4 (8%) cases had PML in which 2 were males and 2 were female patients. On MR imaging, all the cases showed bilateral asymmetrical T2 hyperintense lesions.

On MRS, all 4 cases showed reduced NAA with increased Choline. 2 of the lesions showed lactate peak while 2 cases showed increased myo inositol level within the lesion.

In a study by L. Chang, T. Ernst, C. Tornatore, H. Aronow, R. Melchor, I. Walot, E. Singer, M. Cornford , they found patients with the highest survival had the highest level myoinositol.[48]

NEUROCYSTICERCOSIS

In our study 2 (4%) patients out of 48 had NCC. Both the patients were female patients who had a single well-defined lesion which was T2 hyperintense with no diffusion restriction and peripheral enhancement on contrast scans.

On MRS, both the lesions show reduced NAA with choline peaks.

LIMITATIONS

- Contrast study was not performed in 14 patients as it was not requested by the referring doctor.
- A clear clinical diagnosis could not be established in a few of the cases of encephalitis.
- MR perfusion study and Magnetic transfer imaging which were not included in the study protocol which can be useful in diagnosing various ring enhancing lesions.
- Most of our lesions were performed using multi-voxel techniques which reduced the sensitivity and specificity of MRS due to metabolite bleed in the adjacent voxels.
- Our study did not include any patients under 18 years of age, in whom CNS infections are relatively common.

CONCLUSION

- MRI is a very sensitive modality in the diagnosis and characterization of CNS infections
- MRS are to be routinely used in evaluation of ring enhancing lesions.
- Peripheral/ring enhancement is the most common characteristic feature in well-defined intracranial infections.
- In our study, Encephalitis was the most prevalent infection (25%), followed by Tuberculomas (18%), Pyogenic abscess (14%), Toxoplasmosis (12%), and PML (8%).
- 51-60 years is the most common age group involved (13% of cases) and headache (75%) and vomiting (72%) being the most frequent presenting symptoms.
- 25% of patients presented with a single lesion whereas the 75% presented with multiple lesions with bilateral lesions in 58% of the cases.
- T2, DWI, T1C+ and MRS sequences can help to characterize and differentiate various CNS infections.
- Multiplanar and multiparametric MRI is essential for arriving at a precise diagnosis with identification of accurate anatomical involvement.
- Ring enhancement and lipid-lactate peak on MRS are more in favor of Tuberculoma
- T2 hyperintense lesions with ring enhancement showing amino acid with lactate peaks on MRS indicate pyogenic brain abscesses with increased A/S ratio pointing towards anaerobic etiology.
- Trehalose peak is a relatively specific feature of fungal abscesses.
- Reduced NAA can be a feature of encephalitis, cerebritis, toxoplasmosis, NCC and PML. However, decreased NAA/Cr ratio is specific for encephalitis.
- Increased myoinositol can point towards a diagnosis of PML
- MR spectroscopy is only effective if used as a supplementary imaging technique rather than a standalone technique.

SUMMARY

A prospective observational study was conducted in the department of Radio-Diagnosis of a tertiary care teaching hospital to assess the diagnostic value of MR spectroscopy in central nervous system infections along with use of routine MRI brain.

MRI has turned out to be modality of choice in evaluation of CNS infections in patients with suspected CNS infections since it is a noninvasive modality. It provides an invaluable role in differentiating neoplasm vs infections and adds immense benefit in form of guiding early treatment and intervention.

In this study we came to a conclusion that MR spectroscopy can prove invaluable to accurately diagnose the etiology of CNS infections by studying and comparing the individual metabolite levels and their ratios.

Our study has highlighted the benefits of MR Spectroscopy in diagnosis of CNS infections in a tertiary care hospital. The study findings can be useful for clinicians in early and accurate diagnosis of CNS infections by providing essential metabolite information which in turn will benefit the patient by initiation of early treatment and reduction in morbidity and mortality.

BIBLIOGRAPHY

1. Danielsen ER, Ross B, editors. Magnetic resonance spectroscopy diagnosis of neurological diseases. CRC Press; 1999 Feb 16.
2. Fitch MT, Abrahamian FM, Moran GJ, Talan DA. Emergency department management of meningitis and encephalitis. Infectious disease clinics of North America. 2008 Mar 1;22(1):33-52.
3. Kumar D, Pannu AK, Dhibar DP, Singh R, Kumari S. The epidemiology and clinical spectrum of infections of the central nervous system in adults in north India. Tropical Doctor. 2021 Jan;51(1):48-57.
4. Faghihi R, Zeinali-Rafsanjani B, Mosleh-Shirazi MA, Saeedi-Moghadam M, Lotfi M, Jalli R, Iravani V. Magnetic resonance spectroscopy and its clinical applications: a review. Journal of medical imaging and radiation sciences. 2017 Sep 1;48(3):233-53.
5. Öz G, Alger JR, Barker PB, Bartha R, Bizzi A, Boesch C, Bolan PJ, Brindle KM, Cudalbu C, Dinçer A, Dydak U. Clinical proton MR spectroscopy in central nervous system disorders. Radiology. 2014 Mar;270(3):658-79.
6. Misra UK, Kalita J, Phadke RV, Wadwekar V, Boruah DK, Srivastava A, Maurya PK, Bhattacharyya A. Usefulness of various MRI sequences in the diagnosis of viral encephalitis. Acta Trop. 2010 Dec;116(3):206-11. doi: 10.1016/j.actatropica.2010.08.007. Epub 2010 Sep 9. PMID: 20816658.
7. Grover VP, Tognarelli JM, Crossey MM, Cox IJ, Taylor-Robinson SD, McPhail MJ. Magnetic Resonance Imaging: Principles and Techniques: Lessons for Clinicians. J Clin Exp Hepatol. 2015 Sep;5(3):246-55. doi: 10.1016/j.jceh.2015.08.001. Epub 2015 Aug 20. PMID: 26628842; PMCID: PMC4632105.

8. Chavhan GB. Appropriate selection of MRI sequences for common scenarios in clinical practice. Pediatr Radiol. 2016 May;46(6):740-7. doi: 10.1007/s00247-016-3556-4. Epub 2016 May 26. PMID: 27229493.

9. Grover VP, Tognarelli JM, Crossey MM, Cox IJ, Taylor-Robinson SD, McPhail MJ. Magnetic Resonance Imaging: Principles and Techniques: Lessons for Clinicians. J Clin Exp Hepatol. 2015 Sep;5(3):246-55. doi: 10.1016/j.jceh.2015.08.001. Epub 2015 Aug 20. PMID: 26628842; PMCID: PMC4632105.

10. Sands MJ, Levitin A. Basics of magnetic resonance imaging. Semin Vasc Surg. 2004 Jun;17(2):66-82. doi: 10.1053/j.semvascsurg.2004.03.011. PMID: 15185173.

11. Serai SD. Basics of magnetic resonance imaging and quantitative parameters T1, T2, T2*, T1rho and diffusion-weighted imaging. Pediatr Radiol. 2021 Apr 15. doi: 10.1007/s00247-021-05042-7. Epub ahead of print. PMID: 33856502.

12. Radue EW, Weigel M, Wiest R, Urbach H. Introduction to Magnetic Resonance Imaging for Neurologists. Continuum (Minneap Minn). 2016 Oct;22(5, Neuroimaging):1379-1398. doi: 10.1212/CON.0000000000000391. PMID: 27740981.

13. Skinner S. MRI brain imaging. Aust Fam Physician. 2013 Nov;42(11):794-7. PMID: 24217100.

14. Kurhanewicz J, Vigneron DB, Hricak H, Narayan P, Carroll P, Nelson SJ. Three-dimensional H-1 MR spectroscopic imaging of the in situ human prostate with high (0.24-0.7-cm3) spatial resolution. Radiology. 1996 Mar;198(3):795-805.

15. Faghihi R, Zeinali-Rafsanjani B, Mosleh-Shirazi MA, Saeedi-Moghadam M, Lotfi M, Jalli R, Iravani V. Magnetic resonance spectroscopy and its clinical applications: a review. Journal of medical imaging and radiation sciences. 2017 Sep 1;48(3):233-53.

16. Gaillard, F., Saber, M. MR spectroscopy. Reference article, Radiopaedia.org. (accessed on 02 Dec 2021)

17. Verma A, Kumar I, Verma N, Aggarwal P, Ojha R. Magnetic resonance spectroscopy—revisiting the biochemical and molecular milieu of brain tumors. BBA clinical. 2016 Jun 1;5:170-8.

18. Parikh V, Tucci V, Galwankar S. Infections of the nervous system. International journal of critical illness and injury science. 2012 May;2(2):82.

19. Rath TJ, Hughes M, Arabi M, Shah GV. Imaging of cerebritis, encephalitis, and brain abscess. Neuroimaging Clinics. 2012 Nov 1;22(4):585-607.

20. Jayaraman K, Rangasami R, Chandrasekharan A. Magnetic resonance imaging findings in viral encephalitis: A pictorial essay. Journal of neurosciences in rural practice. 2018 Oct;9(04):556-60.

21 Laubenberger J, Haussinger D, Bayer S, et al. HIVrelated metabolic abnormalities in the brain: depiction with proton MR spectroscopy with short echo times. Radiology 1996;199(3):805–10

22. Chang L, Ernst T, Tornatore C, Aronow H, Melchor R, Walot I, Singer E, Cornford M. Metabolite abnormalities in progressive multifocal leukoencephalopathy by proton magnetic resonance spectroscopy. Neurology. 1997 Apr 1;48(4):836-44.

23. Baburaj R, Rangasami R, Rajakumar PS. Magnetic resonance imaging and magnetic resonance spectroscopy in varicella zoster necrotizing encephalitis. Neurology India. 2018 Jan 5;66(3):836.

24. Britt RH, Enzmann DR. Clinical stages of human brain abscesses on serial CT scans after contrast infusion. Computerized tomographic, neuropathological, and clinical correlations. J Neurosurg 1983;59(6):972–89.

25. Maheshwarappa RP, Agarwal C, Bansal J. Tuberculoma Versus Neurocysticercosis: Can Magnetic Resonance Spectroscopy and Diffusion Weighted Imaging Solve the Diagnostic Conundrum?. Journal of Clinical & Diagnostic Research. 2019 Jun 1;13(6).

26. Suss RA, Maravilla KR, Thompson J. MR imaging of intracranial cysticercosis: comparison with CT and anatomopathologique features. American journal of neuroradiology. 1986 Mar 1;7(2):235-42.

27. Gupta R K, Vatsal DK, Hussain N. Differentiation of tuberculosis from pyogenic brain abscess with in vivo proton MRS. American Journal of Neuroradiology. 2001;22(9):1503-09.

28. Vasudev MK, Jayakumar PN, Srikanth SG, Nagarajan K, Mohanty A. Quantitative magnetic resonance techniques in the evaluation of intracranial tuberculomas. Acta Radiologica. 2007 Jan 1;48(2):200-6.

29. Santhosh NS, Sinha S, Satishchandra P. Epilepsy: Indian perspective. Annals of Indian Academy of Neurology. 2014 Mar;17(Suppl 1):S3.

30. Batra A, Tripathi RP. Diffusion-weighted magnetic resonance imaging and magnetic resonance spectroscopy in the evaluation of focal cerebral tubercular lesions. Acta Radiologica. 2004 Oct;45(6):679-88.

31. Gupta RK, Husain M, Vatsal DK, Kumar R, Chawla S, Husain N. Comparative evaluation of magnetization transfer MR imaging and in-vivo proton MR spectroscopy in brain tuberculomas. Magnetic resonance imaging. 2002 Jun 1;20(5):375-81.

32. Nathal E. Cavernous sinus tuberculoma. Archivos de Neurociencias. 2005;10(1):38-42.

33. Le Son H. Native Vietnamese Medicinal Plants with Anti-atopic Dermatitis Activity: A Systematic Review. Journal of Complementary and Alternative Medical Research. 2016 Dec 13:1-24..

34. Amaral L, Maschietto M, Maschietto R, Cury R, Ferreira NF, Mendonça R, Lima SS. Unusual manifestations of neurocysticercosis in MR imaging: analysis of 172 cases. Arquivos de neuro-psiquiatria. 2003;61:533-41.

35. Kim YJ, Chang KH, Song IC, Kim HD, Seong SO, Kim YH, Han MH. Brain abscess and necrotic or cystic brain tumor: discrimination with signal intensity on diffusion-weighted MR imaging. AJR. American journal of roentgenology. 1998 Dec;171(6):1487-90.

36. Martinez HR, Rangel-Guerra R, Elizondo G, Gonzalez J, Todd LE, Ancer J, Prakash SS. MR imaging in neurocysticercosis: a study of 56 cases. American Journal of Neuroradiology. 1989 Sep 1;10(5):1011-9.

37. Singhal SR, Nanda S, Singhal SK. Neurocysticercosis as an important differential of seizures in pregnancy: two case reports. Journal of medical case reports. 2011 Dec;5(1):1-3.

38. Pal D, Bhattacharyya A, Husain M, Prasad KN, Pandey CM, Gupta RK. In vivo proton MR spectroscopy evaluation of pyogenic brain abscesses: a report of 194 cases. American journal of neuroradiology. 2010 Feb 1;31(2):360-6.

39. Mao J, Li J, Chen D, Zhang J, Wang YJ, Li X, Wang R, Chen LY, Wang XM. Value of MRI in the diagnosis of cerebral abscess caused by Candida albicans in premature infants. Zhongguo Dang dai er ke za zhi= Chinese Journal of Contemporary Pediatrics. 2011 Aug 1;13(8):621-6.

40. Luthra G, Parihar A, Nath K, Jaiswal S, Prasad KN, Husain N, Husain M, Singh S, Behari S, Gupta RK. Comparative evaluation of fungal, tubercular, and pyogenic brain abscesses with conventional and diffusion MR imaging and proton MR spectroscopy. American Journal of Neuroradiology. 2007 Aug 1;28(7):1332-8.

41. Tsuchiya K, Inaoka S, Mizutani Y, Hachiya J. Fast fluid-attenuated inversion-recovery MR of intracranial infections. American journal of neuroradiology. 1997 May 1;18(5):909-13.

42. Shukla-Dave A, Gupta RK, Roy R, Husain N, Paul L, Venkatesh SK, Rashid MR, Chhabra DK, Husain M. Prospective evaluation of in vivo proton MR spectroscopy in differentiation of similar appearing intracranial cystic lesions. Magnetic resonance imaging. 2001 Jan 1;19(1):103-10.

43. Chang KH, Song IC, Kim SH, Han MH, Kim HD, Seong SO, Jung HW, Han MC. In vivo single-voxel proton MR spectroscopy in intracranial cystic masses. American journal of neuroradiology. 1998 Mar 1;19(3):401-5.

44. Gupta RK, Vatsal DK, Husain N, Chawla S, Prasad KN, Roy R, Kumar R, Jha D, Husain M. Differentiation of tuberculous from pyogenic brain abscesses with in vivo proton MR spectroscopy and magnetization transfer MR imaging. American Journal of Neuroradiology. 2001 Sep 1;22(8):1503-9.

45. Robertson FC, Lepard JR, Mekary RA, Davis MC, Yunusa I, Gormley WB, Baticulon RE, Mahmud MR, Misra BK, Rattani A, Dewan MC. Epidemiology of central nervous system infectious diseases: a meta-analysis and systematic review with implications for neurosurgeons worldwide. Journal of neurosurgery. 2018 Jun 15;130(4):1107-26.

46. Pal D, Bhattacharyya A, Husain M, Prasad KN, Pandey CM, Gupta RK. In vivo proton MR spectroscopy evaluation of pyogenic brain abscesses: a report of 194 cases. American journal of neuroradiology. 2010 Feb 1;31(2):360-6.

47. Hitosugi M, Ichijo M, Matsuoka Y, Takenaka N, Fujii H. Proton MR spectroscopy findings in herpes simplex encephalitis. Rinsho shinkeigaku= Clinical neurology. 1996 Jul 1;36(7):839-43.

48. Chang L, Ernst T, Tornatore C, Aronow H, Melchor R, Walot I, Singer E, Cornford M. Metabolite abnormalities in progressive multifocal leukoencephalopathy by proton magnetic resonance spectroscopy. Neurology. 1997 Apr 1;48(4):836-44.

ANNEXURE I

INFORMED CONSENT

TITLE OF THE STUDY: 'MAGNETIC RESONANCE SPECTROSCOPY IN CENTRAL NERVOUS SYSTEM INFECTIONS – A ONE YEAR HOSPITAL BASED OBSERVATIONAL STUDY'

PRINCIPAL INVESTIGATOR:

INTRODUCTION AND PURPOSE:

MR spectroscopy is still considered an "investigational technique" by some medical professionals and health care organizations. However, the ability to make an early, noninvasive diagnosis or to increase confidence in a suspected diagnosis is highly valued by patients and clinicians alike.MR spectroscopy, when combined with routine diagnostic imaging, may provide specific information especially in brain abscess and parasitic infection, which may help in its definitive diagnosis

PROCEDURE:

I request you to kindly participate in the study titled **'MAGNETIC RESONANCE SPECTROSCOPY IN CENTRAL NERVOUS SYSTEM INFECTIONS – A ONE YEAR HOSPITAL BASED OBSERVATIONAL STUDY'** at Dr. Prabhakar Kore charitable hospital and Medical Research Centre, Belgaum" being conducted by post graduate in Radiodiagnosis at J. N. Medical College Belgaum, Karnataka,

We request you to participate in this study as you are eligible to be included. During the study you will be asked questions regarding your present and past medical history and you will be required to answer to the best of your knowledge. You will also be clinically examined as per the protocol drawn.

If you agree to participate in the study please furnish the details pertaining to the study.

BENEFITS:

- Noninvasive modality

COMPLICATIONS

No significant risk to the patient has been documented from MRI Spectroscopy imaging.

ALTERNATIVES:

If a patient is not willing to take part in the study, his / her treatment or any other further investigations the patient wants to undergo, in future, in KLE will not be affected by his / her decision.

VOLUNTARY PARTICIPATION/WITHDRAWAL:

Taking part in this study is voluntary. I may choose not to take part in this study, or if I decide to take part, I can later change my mind and withdraw from the study. My decision will not change the present or future health care or other services that I receive. The study doctor or the sponsor may stop my participation in this study. I will tell you about any important new findings that may change my willingness to continue to take part. If I choose not to take part in the study, I will receive the standard treatment for patients with my condition.

COSTS:

No additional costs other than the MRI which is referred by the consultant for diagnostic purposes.

Payment for Participation: No incentive will be paid to you for participating in this study.

COMPENSATION:

In the event that I become injured as a result of taking part in this study, treatment available at KLE charitable hospital, Belagavi, will be offered to me. No reimbursement, compensation or free medical care is given.

CONFIDENTIALITY:

All information collected about me during the course of the study will be kept confidential to the extent permitted by the law. The code numbers will identify me in this research record. Information from this study may be published but my identity will be confidential in any publication.

CONSENT TO PARTICIPATE IN RESEARCH STUDY:

1. I understand that I am participating in the study, which includes MR Spectroscopy of the brain.
2. I confirm that I have read and understood the information in the patient information sheet. Procedure is explained to me in detail along with information about the advantages and disadvantages of taking part in the study.
3. I understand that the decision to take part in this study is completely voluntary and I am aware that I can choose to withdraw from the study at any point of time.
4. I consent to the photographing or recording of the procedure to be performed including appropriate portions of my body, for medical, scientific or educational purposes provided my identity is not revealed in the pictures or by the descriptive texts accompanying them.
5. I understand that there is no significant risk involved in the test that would be done in this study.
6. My signature on this form signifies that I have willingly decided to participate after understanding the above information.

Participant's Name/ legally authorized representative _____

Signature _____

Name and signature of witness _____

Name and signature of interviewer _____

Date:

Place:

ANNEXURE II

ETHICAL CLEARANCE LETTER

K.L.E. ACADEMY OF HIGHER EDUCATION AND RESEARCH
(Deemed - to-be-University)
Accredited 'A' Grade by NAAC (2nd Cycle) Placed in Category 'A' by MHRD (GoI)
JAWAHARLAL NEHRU MEDICAL COLLEGE,
NEHRU NAGAR, BELAGAVI-590010 (KARNATAKA-INDIA)
Website: http//www.jnmc.edu
E-Mail : dome@jnmc.edu
Phone: (+ 91-(0)831 Office : 2472550
Principal: 2471701
Fax No. +91 (0)831 – 2470759

Ref: MDC/DOME/ 291 **Date: 24/12/2019**

To.
BS0119002
PG student in Radio-diagnosis,
J. N. Medical College,
BELAGAVI.

Sub: Institutional Ethical Clearance for the study.

With reference to the above, we wish to inform you that your proposed research project titled **"ROLE OF MAGNETIC RESONANCE SPECTROSCOPY IN CENTRAL NERVOUS SYSTEM INFECTIONS – A ONE YEAR HOSPITAL BASED OBSERVATIONAL STUDY",** is ethical and justifiable. The proposed research project has been cleared by the JNMC Institutional Ethics Committee on Human Subjects Research.

(Dr. Anita Dalal)
Member Secretary
JNMC Institutional Ethics Committee
on Human Subjects Research,
J.N.Medical College, Belagavi.

(Dr. Roopa M Bellad)
Chairman,
JNMC Institutional Ethics Committee
on Human Subjects Research,
J.N.Medical College, Belagavi.

ANNEXURE III

S. No:

PROFORMA FOR DATA COLLECTION

NAME: _____

AGE :_____

OP/IP NO : _____

MOBILE NO :_____

ADDRESS: _____

_____

MRI NUMBER: _____

CHIEF COMPLAINTS:

HISTORY OF PRESENTING ILLNESS:

OTHER RELEVANT HISTORY IF ANY:

ROUTINE MRI & SPECTROSCOPY FINDINGS:

ANNEXURE IV

MRI CASE IMAGES

IMAGE 1-ASHOK HADIMANI

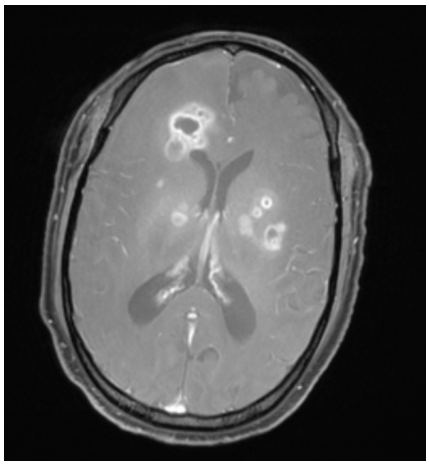

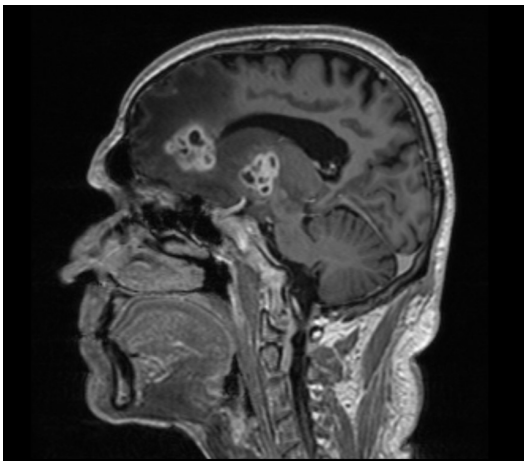

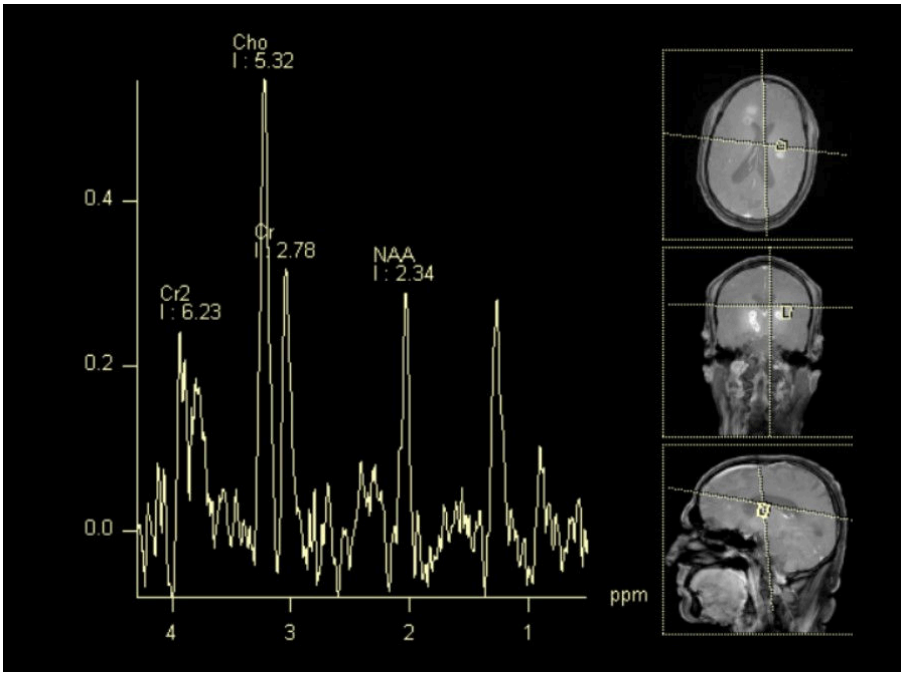

- Multiple well-defined conglomerated T2 hypointense ring enhancing lesions with lipid-lactate peak suggestive of cryptococcoma.

IMAGE 2- GIRIJA

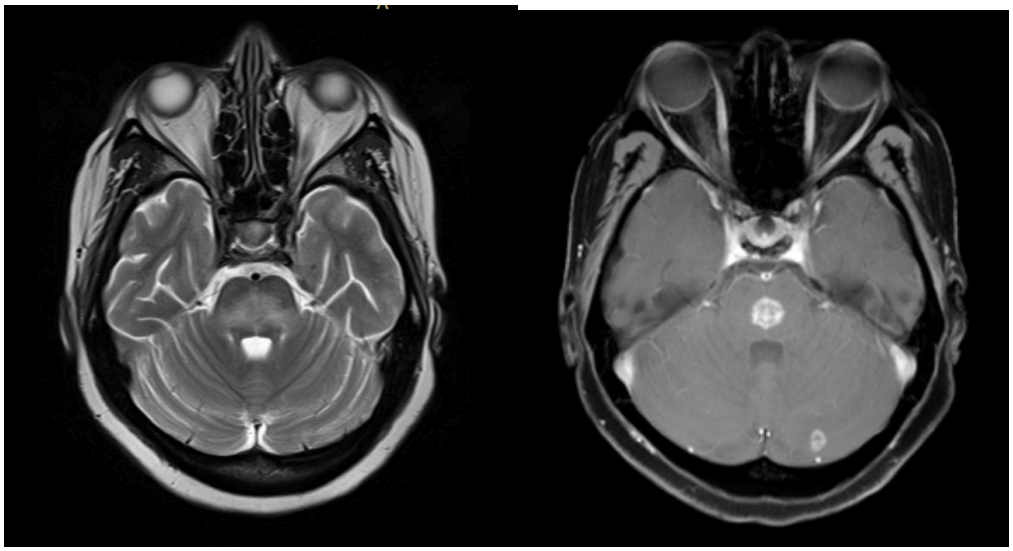

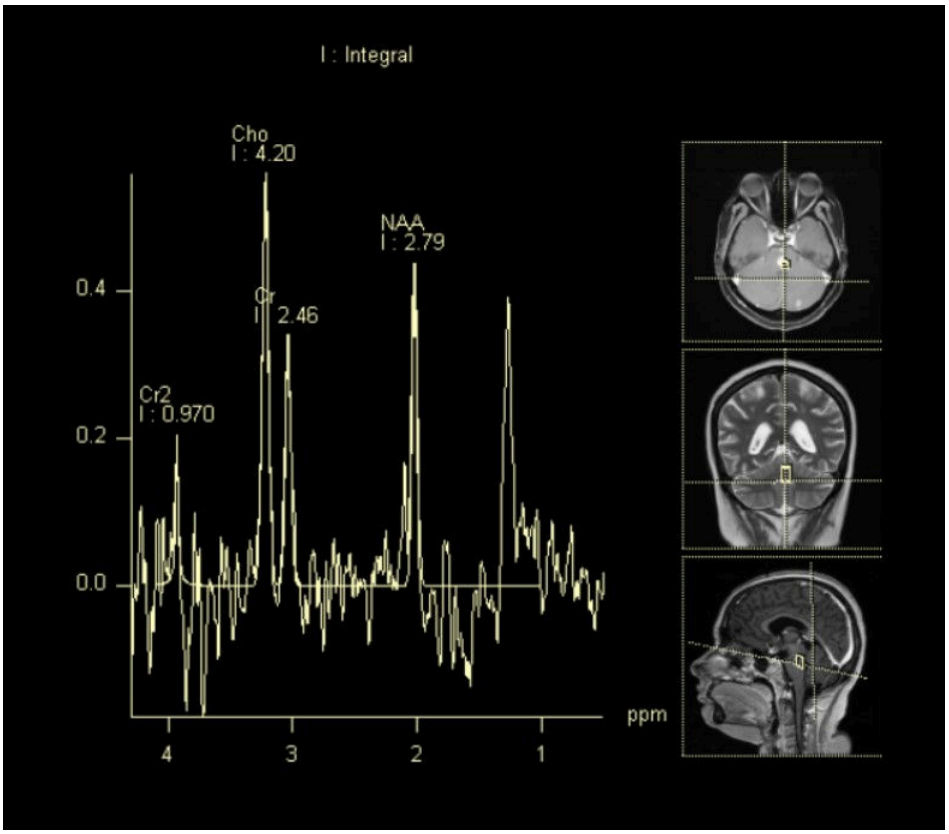

- Few T2 hyperintense ring enhancing lesions showing LL peak and reduced NAA suggestive of toxoplasmosis.

IMAGE 3- ISHANAVI

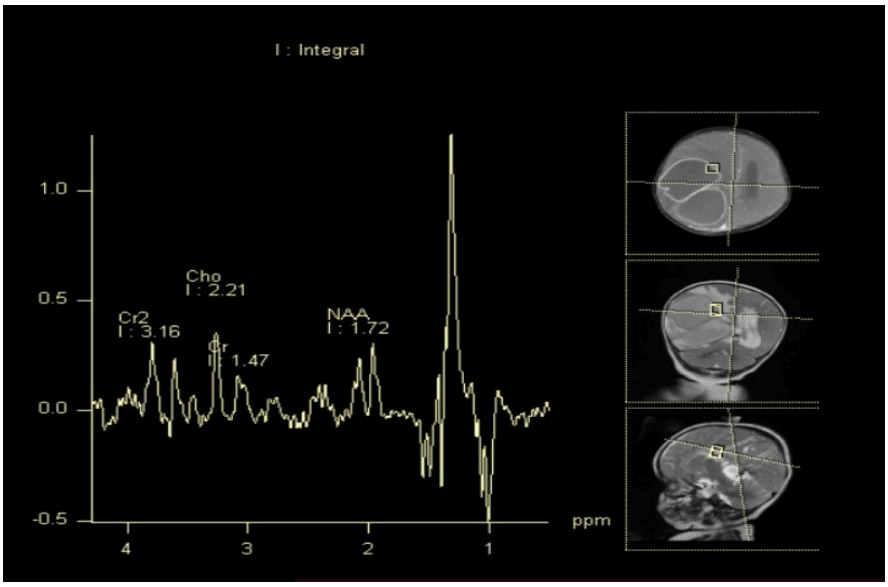

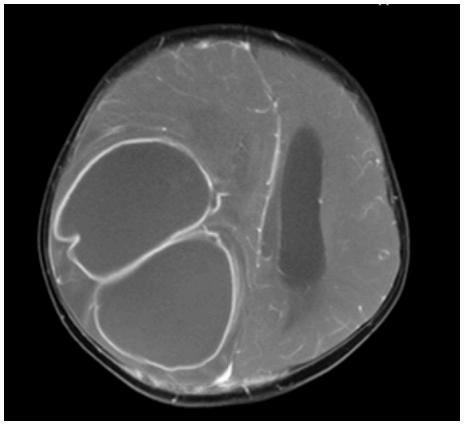

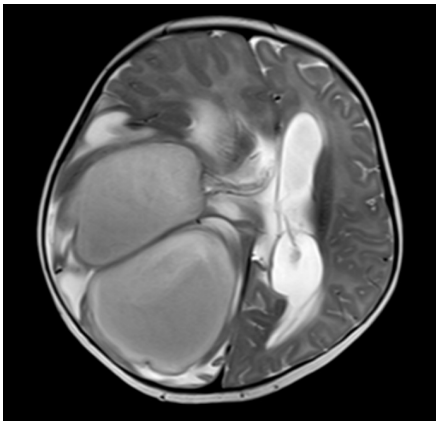

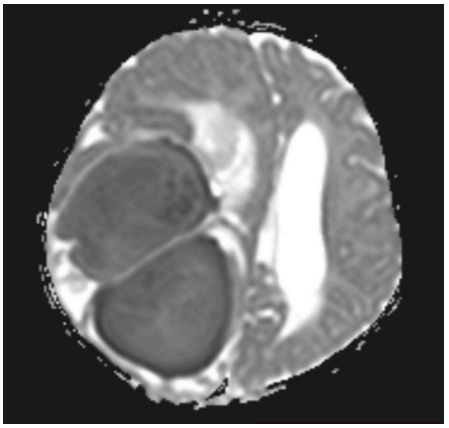

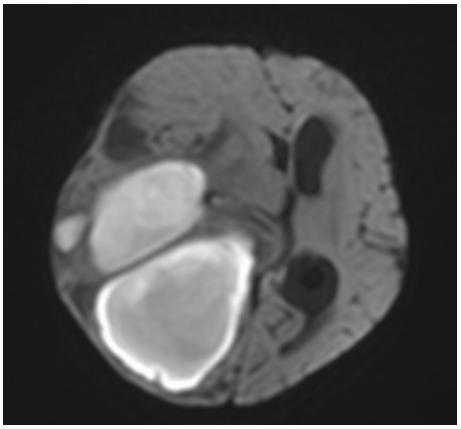

- Few large T2 hyperintense lesion with perilesional edema, diffusion restriction and ring enhancement showing Lipid lactate peak suggestive bacterial abscesses.

IMAGE 4- LALAPPA

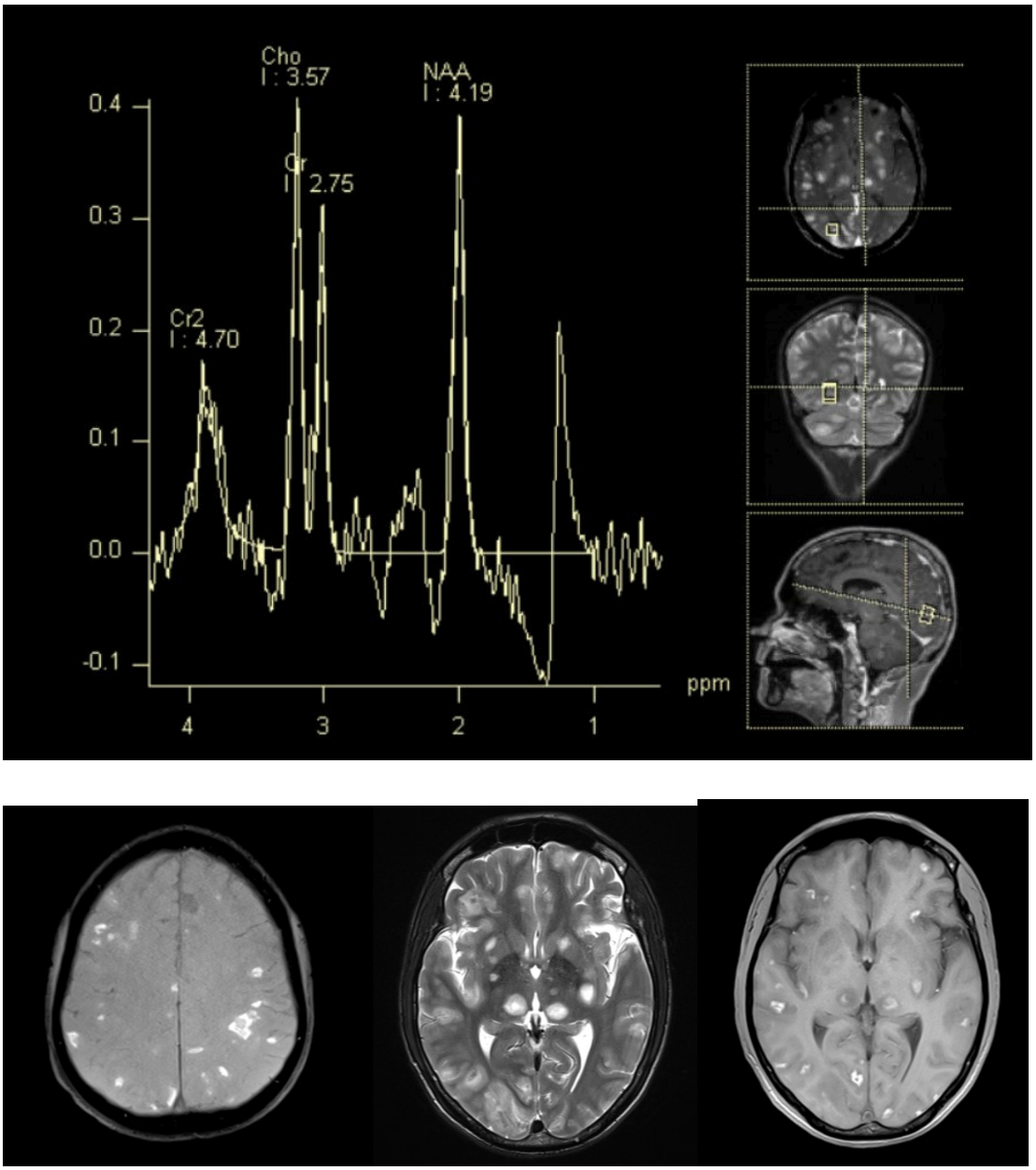

- Multiple ring enhancing conglomerated T1 and T2 hyperintense lesions showing raised choline with lipid lactate peak suggestive of toxoplasmosis.

IMAGE 5- MAHADEVI

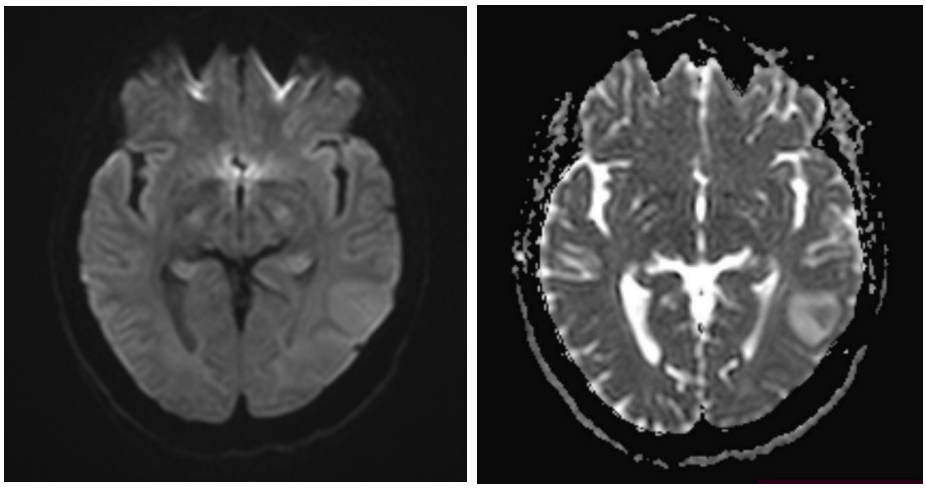

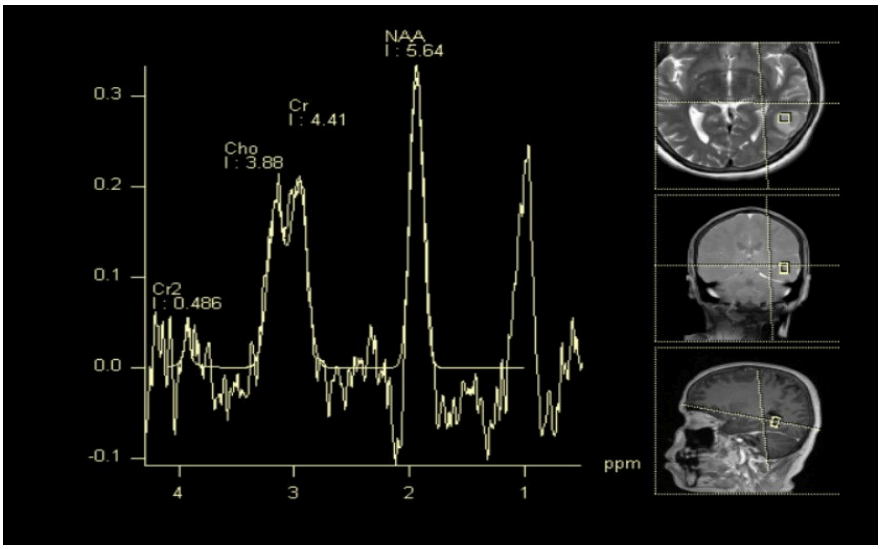

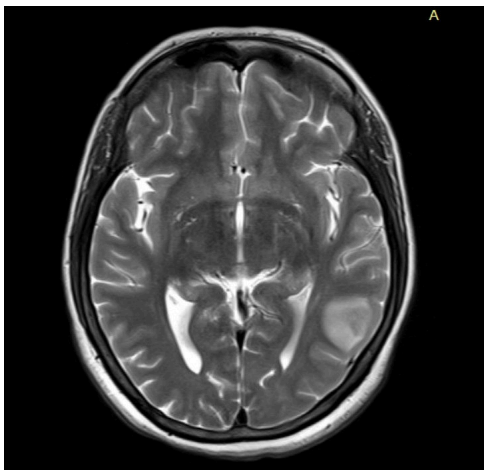

- Ill-defined T2 hyperintense lesion with diffusion restriction showing lipid lactate peak with reduced NAA suggestive of tuberculoma

IMAGE 6- RAMESH

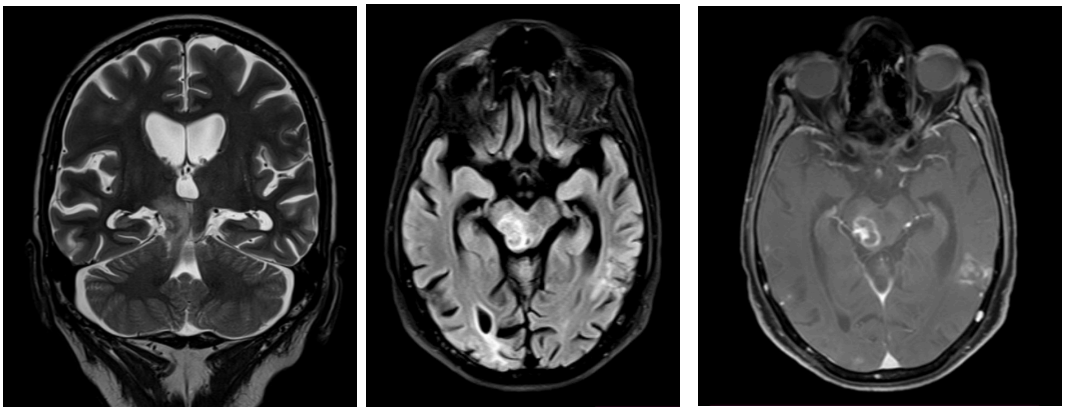

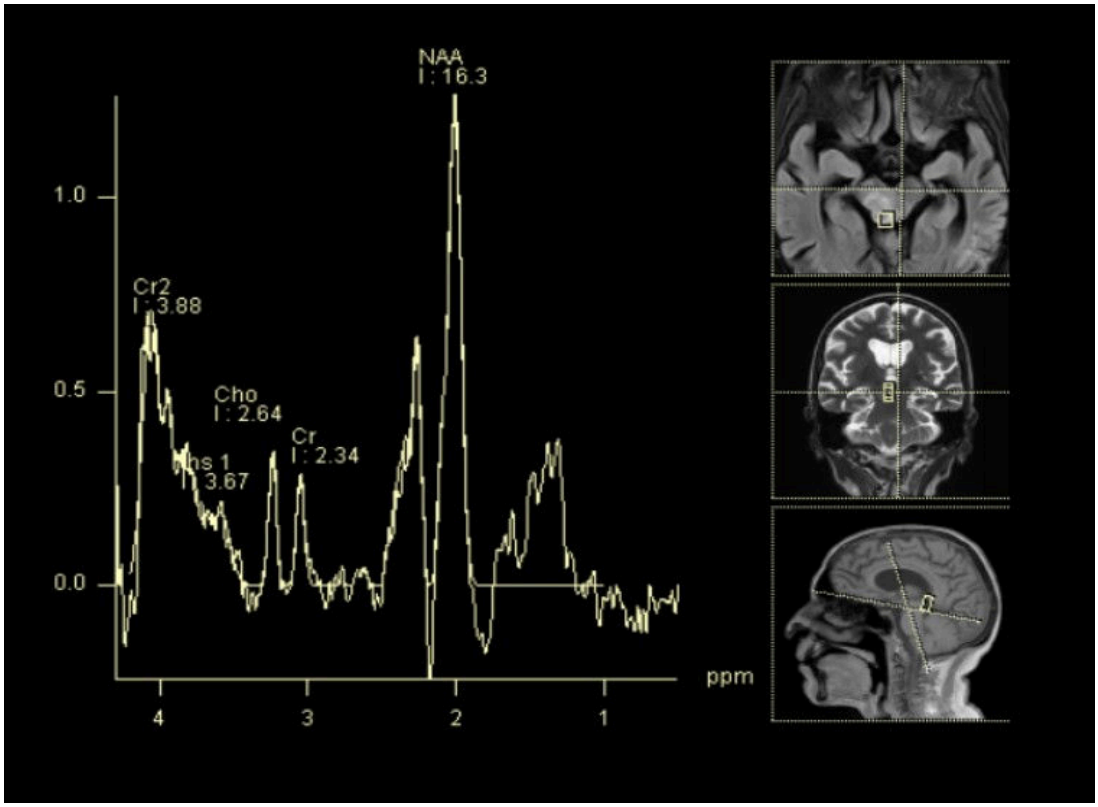

- Few T2 hyperintense ring enhancing lesions showing nodular enhancement so toxoplasmosis.

IMAGE 7- MAHIBUBA

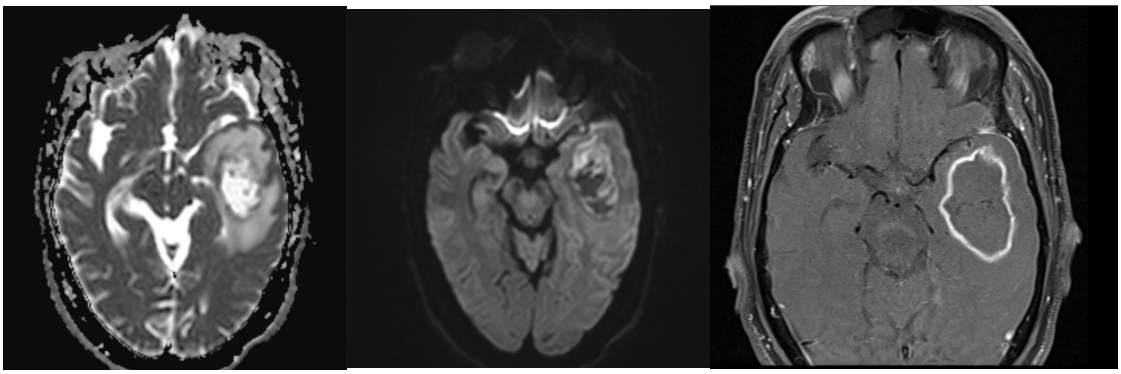

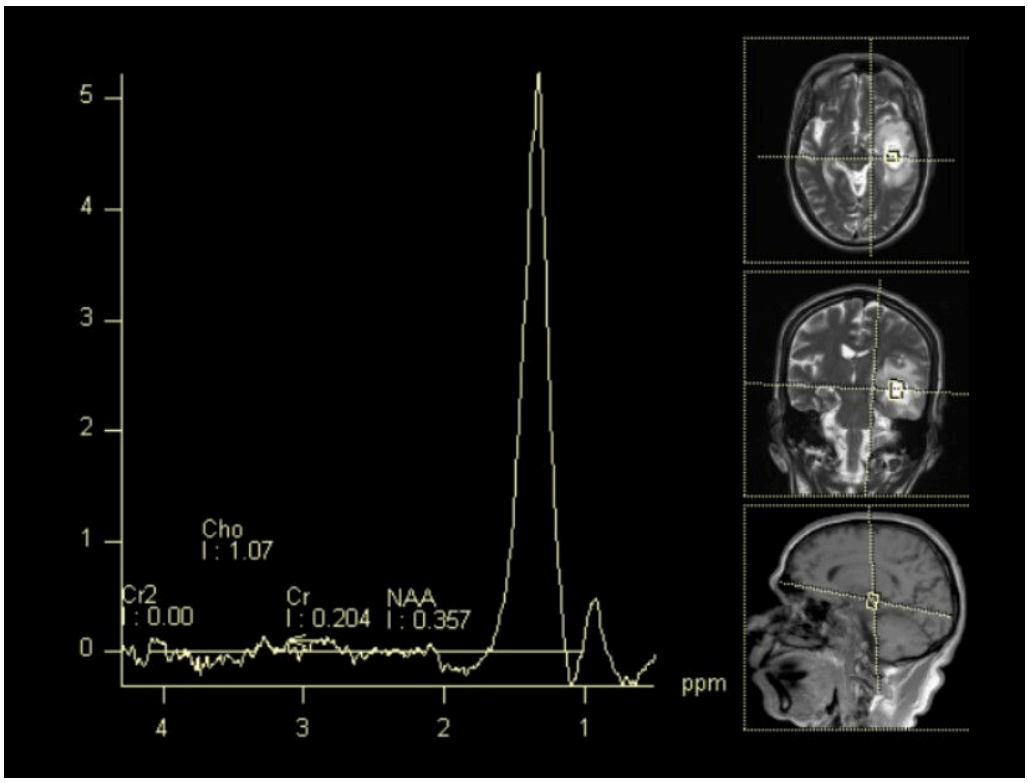

- A large peripherally enhancing T2 hyperintense lesion showing diffusion restriction and showing a lactate and AA peak suggestive of a fungal abscess.

IMAGE 8- MALLIKARJUN

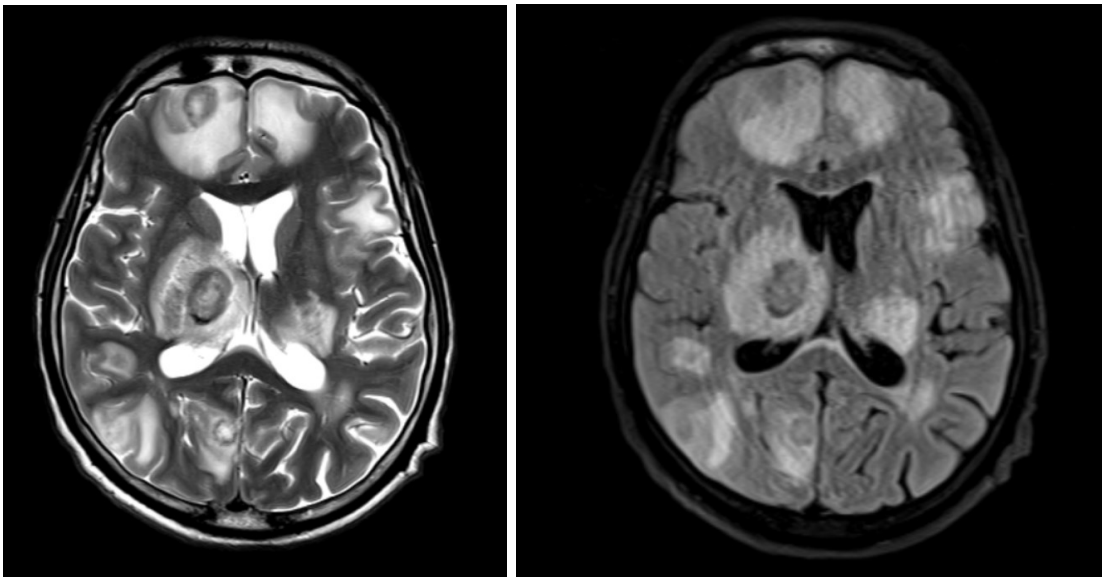

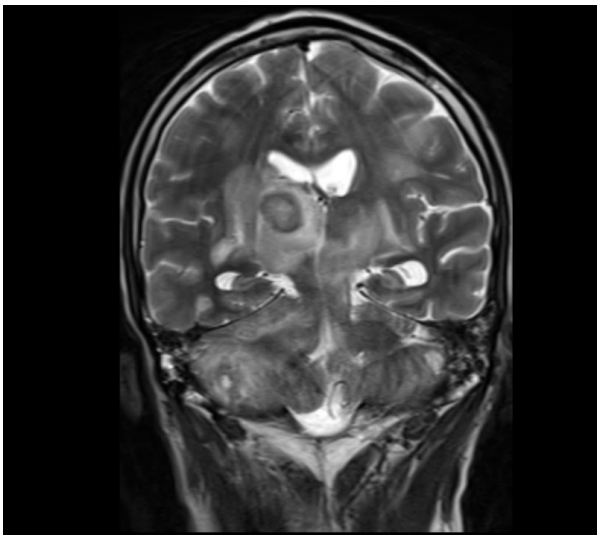

- Multiple T2 peripherally hypointense lesions showing peripheral diffusion restriction with reduced NAA/Cr ratio and a LL peak suggestive of tuberculoma.

IMAGE 9- MALU S

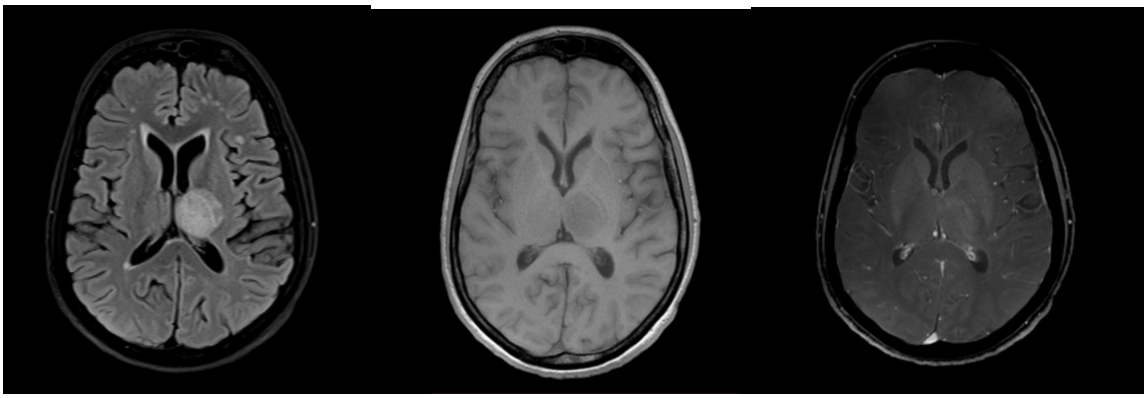

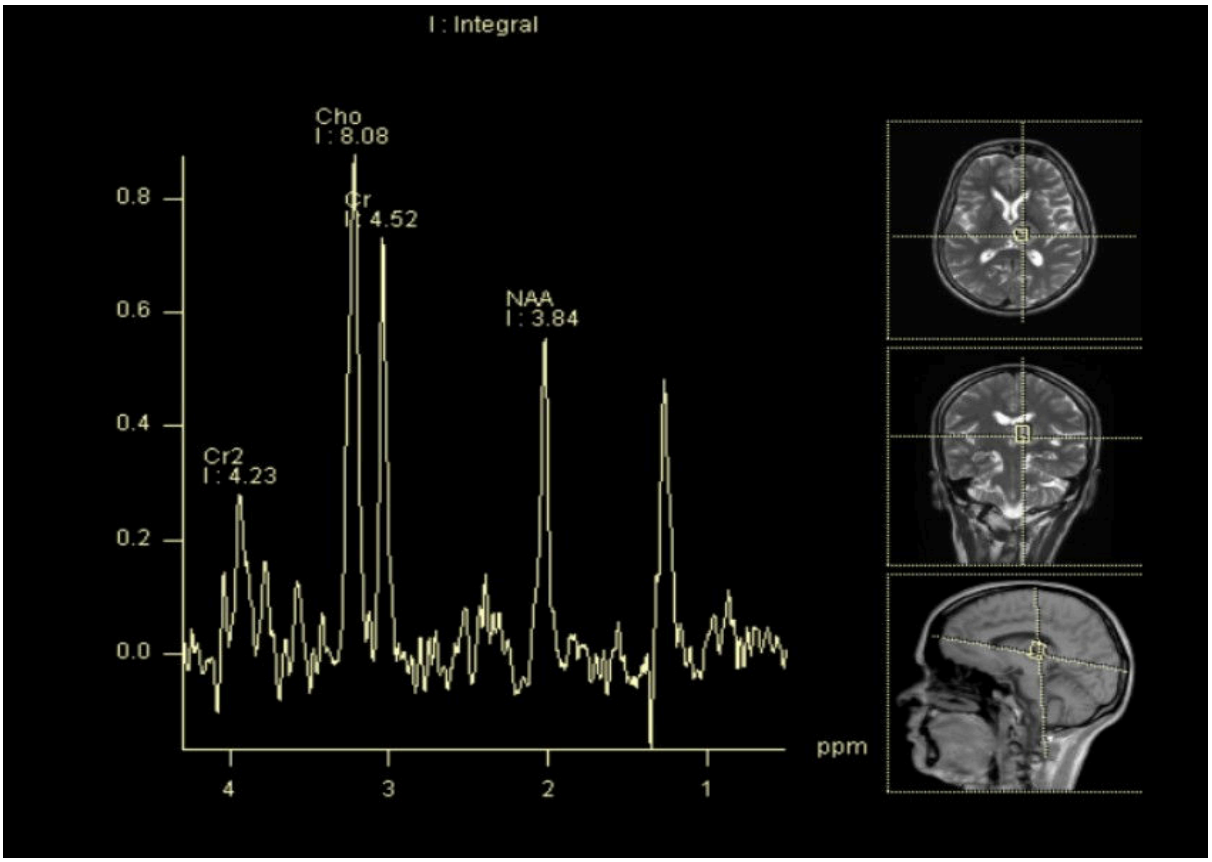

- Mildly enhancing T2 hyperintense lesion in the left thalamus with reduced NAA and decreased NAA/Cr ratio suggestive of encephalitis

IMAGE 10- POOJA

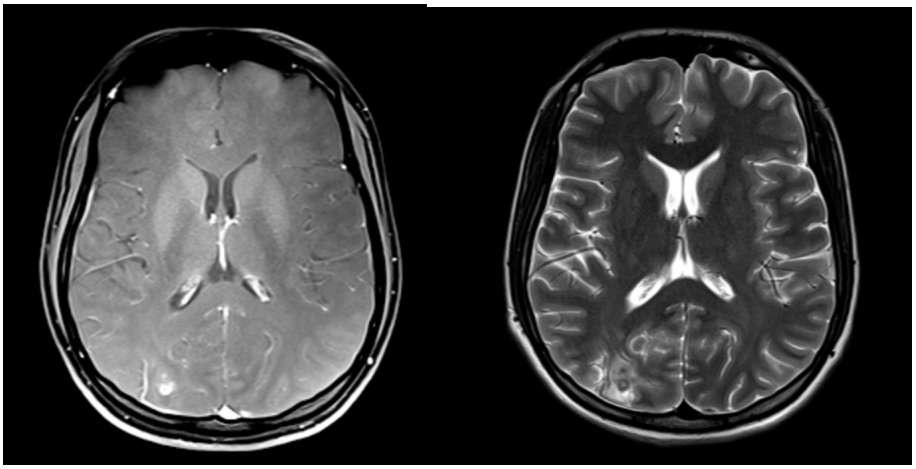

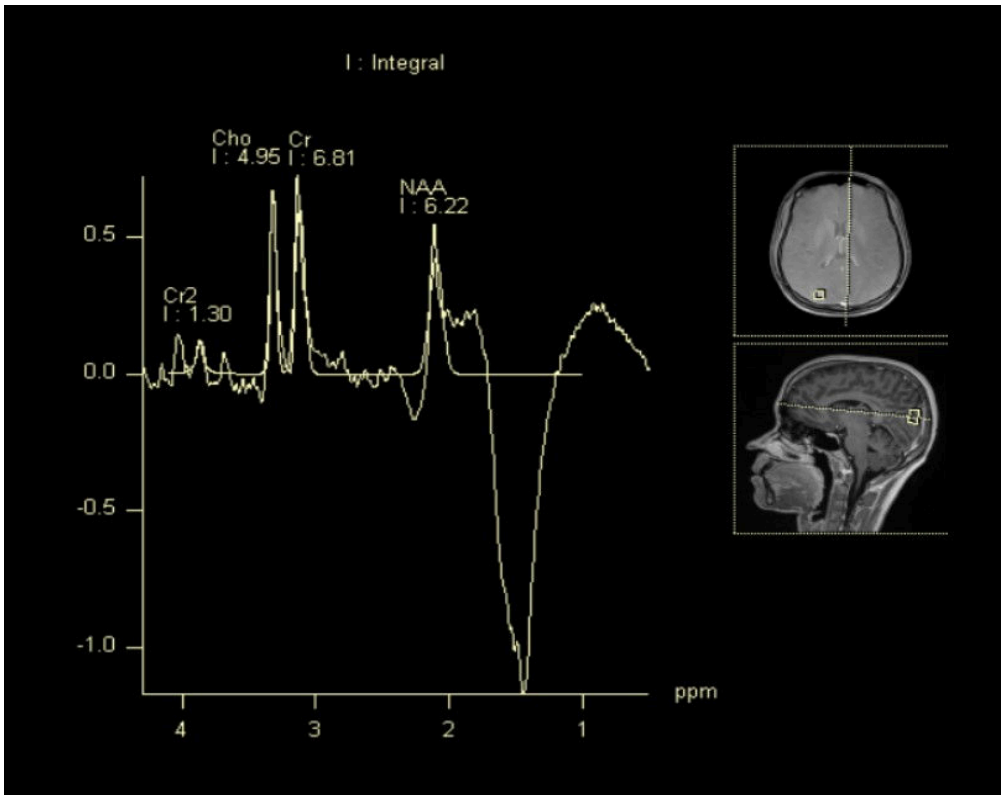

- Peripherally enhancing T2 hyperintense lesion showing reduced NAA with lactate peak suggestive of toxoplasmosis.

IMAGE 11- REKHA

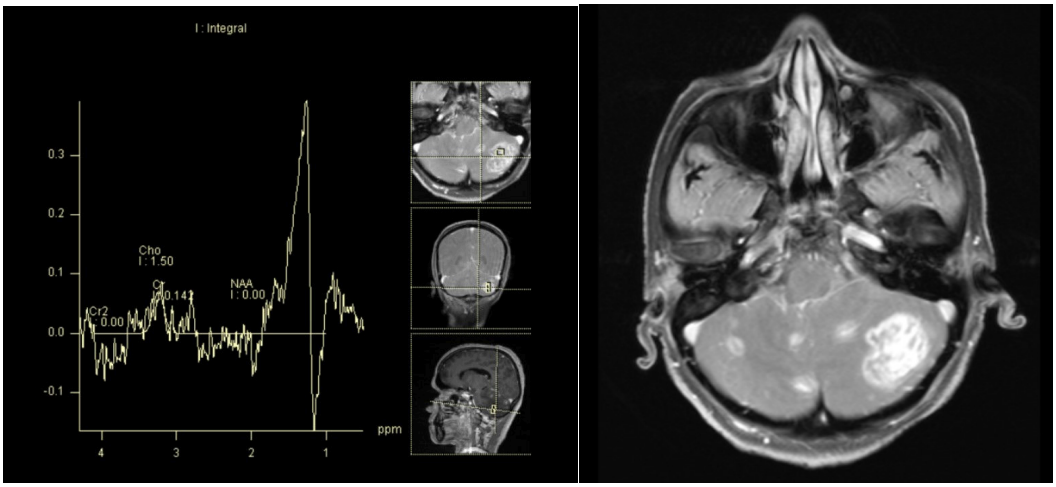

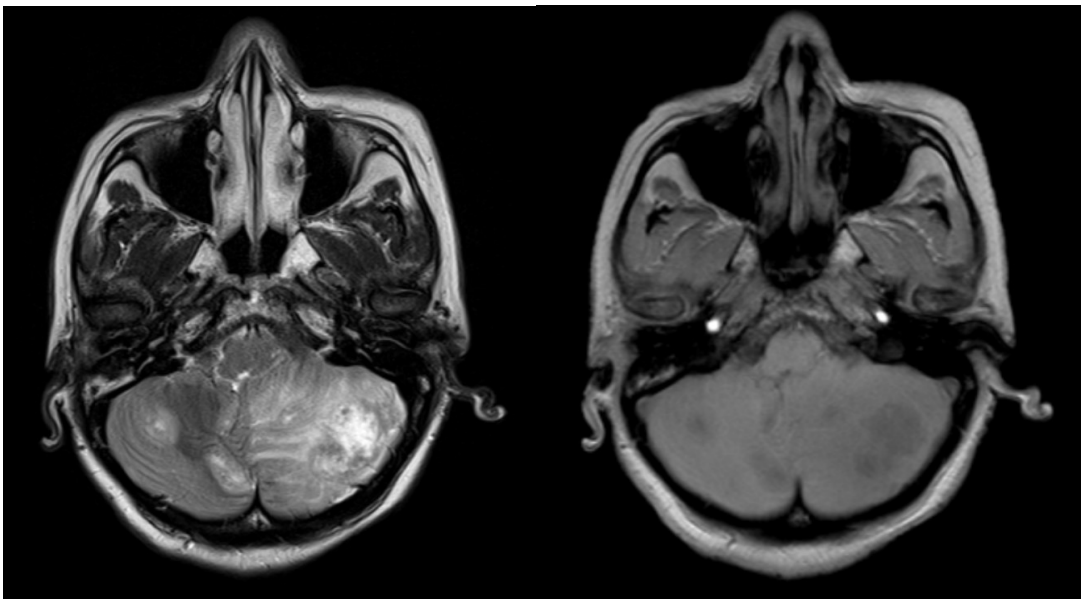

- Multiple T2 hyperintense ring enhancing lesions showing eccentric target sign with LL peak suggestive of toxoplasmosis.

IMAGE 12- SAMYUKTA

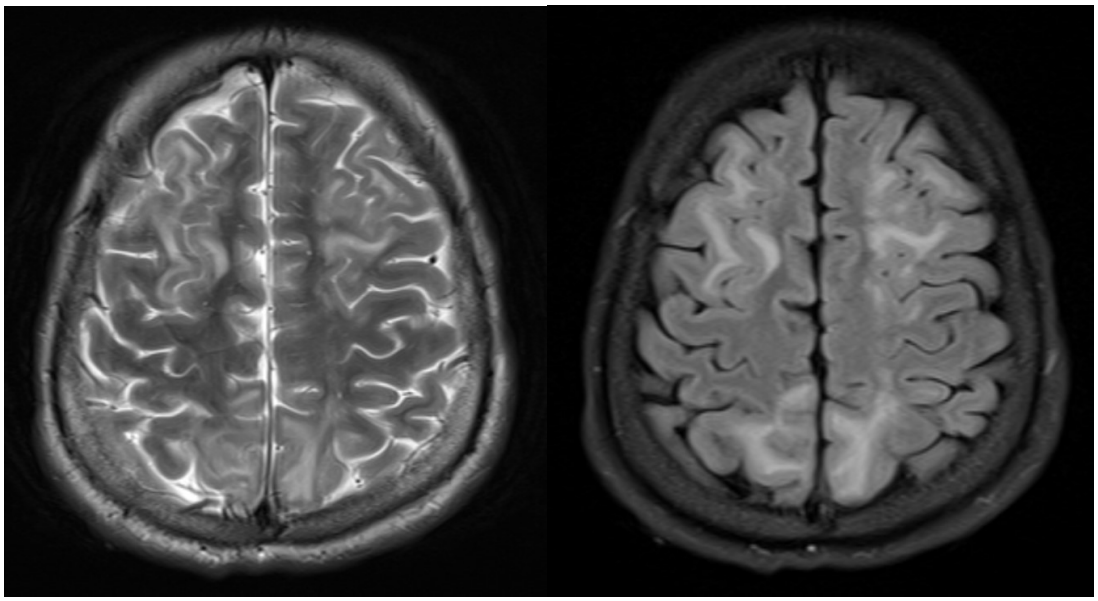

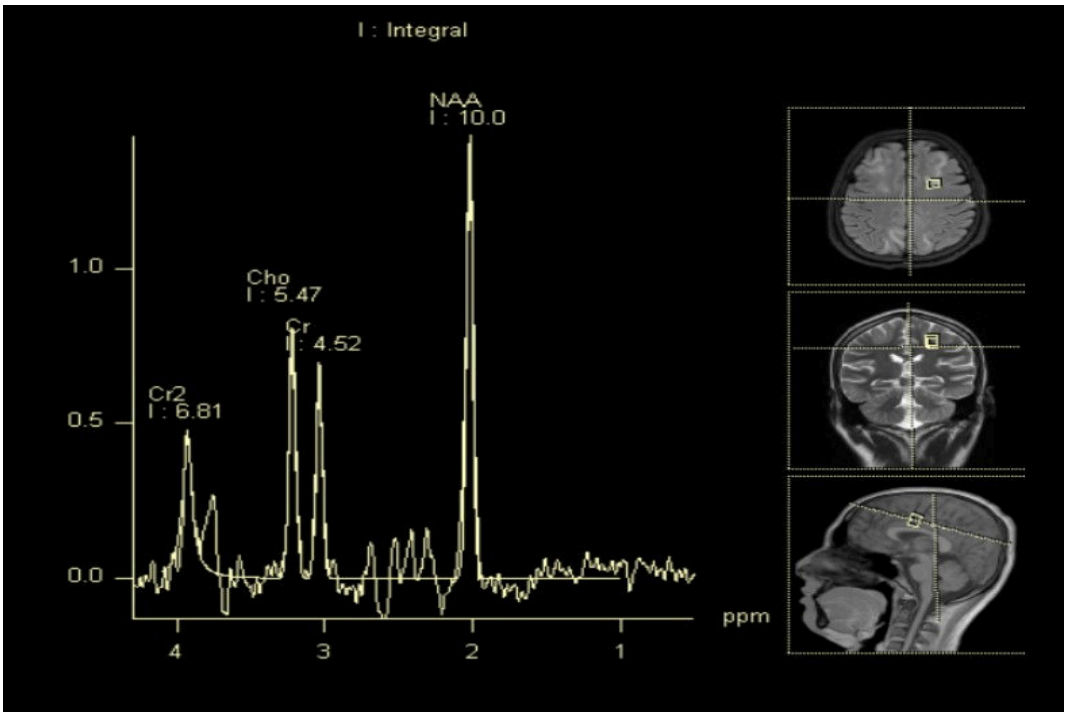

- Symmetrical T2 and FLAIR hyperintensities in bilateral frontal regions with absent diffusion restriction and normal spectroscopy suggestive encephalitis.

IMAGE 13- VIJETHA

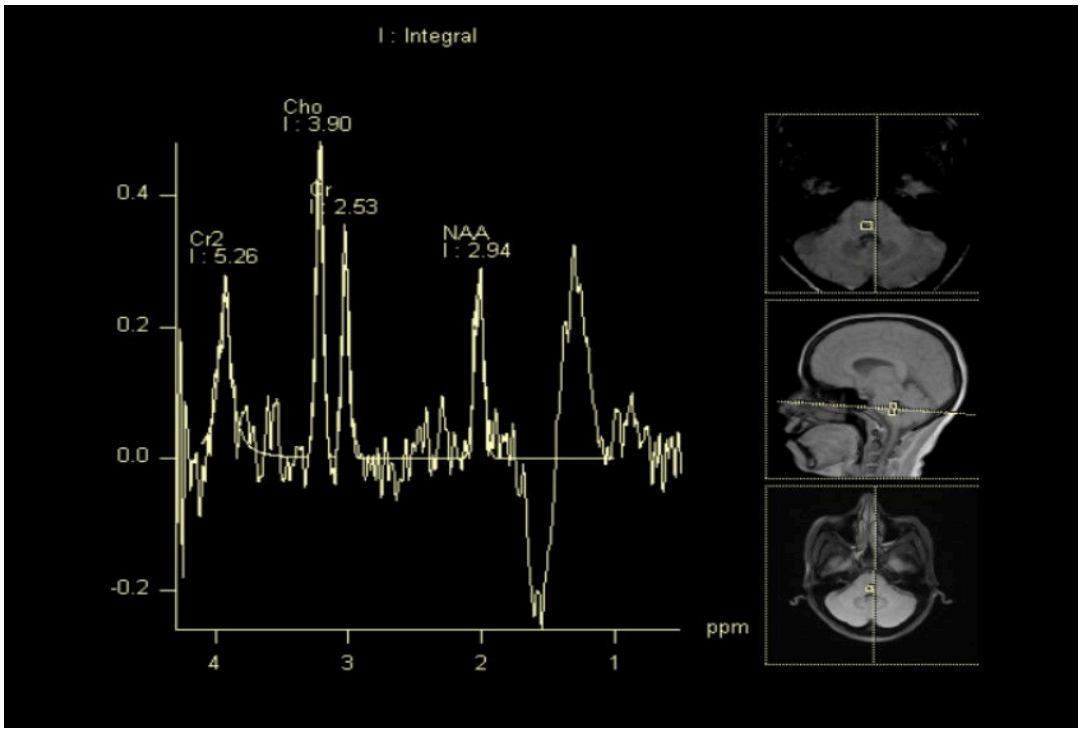

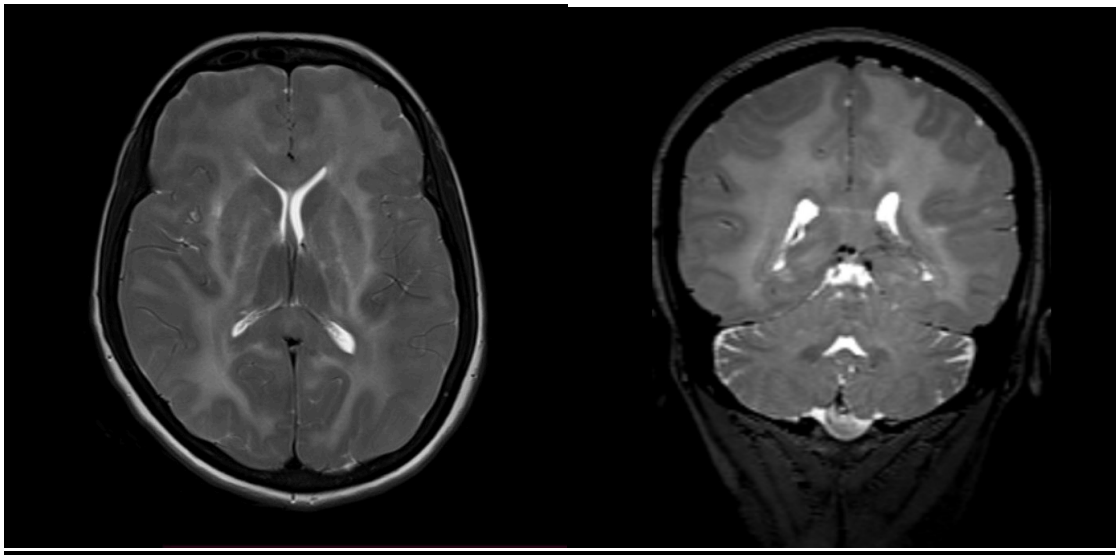

- Bilaterally symmetrical T2 and FLAIR hyperintensities with reduced NAA on spectroscopy suggestive HIV encephalitis.

ANNEXURE V

KEY TO MASTER CHART

M- Male

F-Female

N/A-Not available

i- Increased

r- Reduced

LL- Lipid lactate

Ac - Acetate

Gly- Glycine

A/S- Acetate/Succinate

NAA- N-acetyl aspartate

Cr-Creatine

Ala- Alanine

Cho- Choline

Myo- Myoinositol

AA- Amino acid

Tre- Trehalose

Glx-Glutamine- Glutamate- GABA complex

Lac- Lactate

MRS- Magnetic Resonance spectroscopy

Lip- Lipid

ANNEXURE VI MASTER CHART

NO.	NAME	AGE	SEX	SYMPTOMS	SIDE OF LESION	LESION LOCATION	NUMBER OF LES	MARGINS	SYMMETRY	T1 MORPHOLOGY	T2 MORPHOLOGY	DIFFUSION RESTRICTION	T1 C+ FS	MRS	RADIOLOGICAL DIAGNOSIS
1	ABDUL GIRUKAR	61	M	HEADACHE	RIGHT	FRONTAL REGION	4	WELL DEFINED	-	HYPERINTENSE	HYPOINTENSE	CENTRAL RESTRICTION	RING ENHANCING	LL peak	BACTERIAL ABSCESS
3	ANAND UMARANI	40	M	HEADACHE, NASAL BLOCKAGE WITH DISCHARGE	LEFT	FRONTAL REGION	1	WELL DEFINED	-	ISO	MIXED	PERIPHERAL RESTRICTION	N/A	iAc, LL peak, iGly, iA/S ratio	BACTERIAL ABSCESS
4	ANANTHMURTHY GUDI	29	M	HEADACHE, FEVER, VOMITING, ALTERED SENSORIUM	RIGHT	PARIETAL REGION	2	WELL DEFINED	-	ISOINTENSE	HYPO INTENSE	ABSENT DIFFUSION RESTRICTION	RING ENHANCING	rNAA/Cr, LL peak	TUBERCULOMA (HIV)
2	ASHOK HADIMANI	51	M	HEADACHE, FEVER, VOMITING	BILATERAL	BASAL GANGLIA	MULTIPLE	WELL DEFINED	-	HYPOINTENSE	HYPOINTENSE	CENTRAL RESTRICTION	N/A	iTre, rNAA, rCr	CRYPTOCOCCOMA (HIV)
5	BASAPPA PATIL	49	M	HEADACHE, FEVER, VOMITING, ATAXIA	LEFT	FRONTAL REGION	1	WELL DEFINED	-	HYPOINTENSE	HYPERINTENSE	ABSENT DIFFUSION RESTRICTION	RING ENHANCING	iAc, iAla, LL peak, iA/S ratio	BACTERIAL ABSCESS
6	BASAYYA HIREMATH	27	M	HEADACHE, FEVER, SEIZURES	LEFT	FRONTAL REGION	1	WELL DEFINED	-	HYPERINTENSE	HYPOINTENSE	ABSENT DIFFUSION RESTRICTION	RING ENHANCEMENT	LL peak	TUBERCULOMA
7	BHARAT KUMBAR	60	M	HEADACHE, VOMITING, ATAXIA, ALTERED SENSORIUM	BILATERAL	CEREBELLAR LOBES	MULTIPLE	ILL DEFINED	-	ISOINTENSE	HYPOINTENSE	ABSENT DIFFUSION RESTRICTION	N/A	r NAA, rNAA/Cr ratio	CEREBELLITIS
8	CHANDRAKANT BADAMJI	60	M	HEADACHE, FEVER, VOMITING, SEIZURES	LEFT	FRONTAL REGION, GYRI IN TEMPORAL REGION	MULTIPLE	WELL DEFINED	-	HYPOINTENSE	HYPERINTENSE	DIFFUSION RESTRICTION	PERIPHERAL ENHANCING, LEF	iAc, iAla, , iSch, LL peak, nor	BACTERIAL ABSCESS WITH MENINGI
9	DHANAVVA	60	F	HEADACHE, FEVER, SEIZURES, MOTOR WEAKNESS	BILATERAL	FRONTAL, INSULAR, TEMPORAL, RIGHT CINGULAT	MULTIPLE	ILL DEFINED	-	HYPOINTENSE	HYPERINTENSE	ABSENT DIFFUSION RESTRICTION	N/A	rNAA/Cr, iCho/Cr ratio	HSV ENCEPHALITIS
10	GANPATI CHOUGULE	50	M	FEVER, VOMITING	BILATERAL	TEMPORAL REGIONS	MULTIPLE	ILL DEFINED	+	HYPOINTENSE	HYPERINTENSE	ABSENT DIFFUSION RESTRICTION	N/A	rNAA/Cr	HSV ENCEPHALITIS
11	GIRIJA HALPANNAVAR	38	F	HEADACHE ATAXIA, SEIZURES, ALTERED SENSORIUM	BILATERAL	BASAL GANGLIA	2	WELL DEFINED	+	ISOINTENSE	HYPERINTENSE	ABSENT DIFFUSION RESTRICTION	RING ENHANCING	LL peak, rNAA	TOXOPLASMOSIS
12	GURRPADAPPA AGASIBAG	76	M	HEADACHE, FEVER, VOMITING, SEIZURES	LEFT	PARIETAL REGION	MULTIPLE	ILL DEFINED	-	HYPOINTENSE	HYPERINTENSE	DIFFUSION RESTRICTION	ENHANCING	NORMAL	MENINGOENCEPHALITIS
13	ISHANAVI MUGABASAV	18	F	HEADACHE, FEVER, VOMITING	RIGHT	PARITOTEMPOROOCCIPITAL REGIONS	2	WELL DEFINED	-	HYPOINTENSE	HYPERINTENSE	CENTRAL RESTRICTION	RING ENHANCING	LL peak	BACTERIAL ABSCESS
14	JAYAWANT PATIL	51	M	FEVER, VOMITING	LEFT	BASAL GANGLIA	1	WELL DEFINED	-	HYPOINTENSE	HYPERINTENSE	ABSENT DIFFUSION RESTRICTION	PERIPHERAL ENHANCING	LL peak, rNAA	TOXOPLASMOSIS
15	JINNAPPA K	56	M	HEADACHE, FEVER, VOMITING, ATAXIA	BILATERAL	PERIVENTRICULAR AND FRONTAL REGIONS	MULTIPLE	ILL DEFINED	-	ISOINTENSE	HYPER INTENSE	ABSENT DIFFUSION RESTRICTION	N/A	rNAA, iCho, i myo, LL peak	PML (HIV+)
16	LALAPPA MADAR	45	M	HEADACHE, FEVER, ALTERED SENSORIUM	BILATERAL	SUPRATENTORIAL AND INFRATENTORIAL REGION	MULTIPLE	WELL DEFINED	-	HYPERINTENSE	HYPERINTENSE	ABSENT DIFFUSION RESTRICTION	RING ENHANCING	iCho, LL peak	TOXOPLASMOSIS (HIV)
17	MAHADEV AANI	52	M	HEADACHE, FEVER, VOMITING	BILATERAL	PERITRIGONAL REGIONS AND FRONTOPARIETAL F	MULTIPLE	ILL DEFINED	-	ISOINTENSE	HYPERINTENSE	PERIPHERALRESTRICTION	N/A	rNAA, iCho, i myo, LL pe	PML
18	MAHADEVI TAKEKAR	46	F	HEADACHE, VOMITING, ATAXIA, MOTOR WEAKNESS	BILATERAL	FRONTAL AND TEMPORAL	4	WELL DEFINED	-	ISOINTENSE	HYPERINTENSE	DIFFUSION RESTRICTIONC	RING ENHANCING	rNAA/Cr	CHRONIC TUBERCULOSIS
19	MAHIBULLA MULLA	62	M	FEVER, VOMITING, ATAXIA, SEIZURES	LEFT	TEMPORAL REGIONS	1	WELL DEFINED	-	HYPOINTENSE	HYPERINTENSE	PERIPHERAL RESTRICTION	PERIPHERAL +	AA peak	FUNGAL ABSCESS WITH MENINGITIS
20	MALLAVVA KALLUR	50	F	HEADACHE	BILATERAL	INSULAR CORTEX, GYRA ALONG FRONTOPARIETA	MULTIPLE	ILL DEFINED	-	ISOINTENSE	HYPERINTENSE	DIFFUSION RESTRICTION	N/A	rNAA/Cr, iCho/Cr ratio	HSV ENCEPHALITIS
24	MALLAWA KALLUR	50	F	HEADACHE, VESICULAR RASHES	BILATERAL	INSULAR CORTEX, FRONTOPARIETAL REGIONS	MULTIPLE	ILL DEFINED	-	ISOINTENSE	HYPERINTENSE	DIFFUSION RESTRICTION	N/A	rNAA/Cr	HSV ENCEPHALITIS
22	MALLIKARJUN HIREMATH	61	M	HEADACHE, FEVER, VOMITING, ATAXIA	RIGHT	FRONTAL REGION	5	WELL DEFINED	-	ISOINTENSE	HYPERINTENSE	DIFFUSION RESTRICTION	RING ENHANCING	iTre, LL peak	FUNGAL ABSCESS (MUCOR)
23	MALLIKARJUN MAGADUM	35	M	FEVER, VOMITING, ALTERED SENSORIUM	BILATERAL	SUPRATENTORIAL AND INFRATENTORIAL REGION	MULTIPLE	WELL DEFINED	-	ISOINTENSE	PERIPHERALLY HYPOI	PERIPHERAL RESTRICTION	N/A	rNAA/Cr, LL peak	TUBERCULOMAS
21	MALU SAMBHAJICHE	53	F	FEVER, VOMITING, SEIZURES	LEFT	BASAL GANGLIA, TEMPORAL REGION	2	WELL DEFINED	-	ISOINTENSE	HYPERINTENSE	ABSENT DIFFUSION RESTRICTION	ENHANCING	iGlx, iLac	ENCEPHALITIS
25	MANJULA RACHGANI	26	F	FEVER, VOMITING	LEFT	PARIETAL REGION	1	WELL DEFINED	-	HYPOINTENSE	HYPERINTENSE	ABSENT DIFFUSION RESTRICTION	RING ENHANCEMENT	rNAA, iCho	NCC
26	MANOHAR	52	M	FEVER, VOMITING	LEFT	FRONTAL REGION	1	WELL DEFINED	-	ISOINTENSE	HYPERINTENSE	DIFFUSION RESTRICTION	N/A	LL peak	TUBERCULOMA
27	MONICA	30	F	FEVER, VOMITING	BILATERAL	MEDIAL TEMPORAL REGIONS, INSULAR CORTEX	MULTIPLE	ILL DEFINED	+	ISOINTENSE	HYPERINTENSE	DIFFUSION RESTRICTION	LEPTOMENINGEAL ENHANCE	NORMAL	HSV ENCEPHALITIS
28	PARVATI BHIMGOL	60	F	HEADACHE, FEVER, VOMITING	LEFT	FRONTAL REGION	1	WELL DEFINED	-	HYPOINTENSE	HYPERINTENSE	ABSENT DIFFUSION RESTRICTION	RING ENHANCEMENT	rNAA, iCho	NCC
29	POOJA BISURE	26	F	HEADACHE	RIGHT	PARIETAL AND OCCPITAL REGION	4	WELL DEFINED	-	HYPERINTENSE	HYPOINTENSE	ABSENT DIFFUSION RESTRICTION	RING ENHANCEMENT	LL peak	TUBERCULOMA
30	RAMESH NISURGE	42	M	HEADACHE, FEVER, VOMITING, SEIZURES	LEFT	BASAL GANGLIA, BRAINSTEM	4	WELL DEFINED	-	ISOINTENSE	HYPERINTENSE	PERIPHERAL RESTRICTION	PERIPHERAL ENHANCING	LL peak, rNAA	TOXOPLASMOSIS
31	REKHA KALAGADE	35	F	FEVER, VOMITING	BILATERAL	SUPRATENTORIAL AND INFRATENTORIAL REGION	MULTIPLE	WELL DEFINED	-	ISOINTENSE	HYPERINTENSE	ABSENT DIFFUSION RESTRICTION	RING ENHANCEMENT	LL peak, rNAA	TOXOPLASMOSIS (HIV)
32	SADASHIV R	20	M	HEADACHE, FEVER, ALTERED SENSORIUM	BILATERAL	SUPRATENTORIAL, BRAINSTEM AND INFRATENTO	MULTIPLE	WELL DEFINED	-	HYPOINTENSE	MIXED LAMELLATED	PERIPHERAL RESTRICTION	RING ENHANCEMENT	LL peak	TOXOPLASMOSIS
33	SAMYUKTA KAMALPUTRE	58	M	HEADACHE, FEVER, ATAXIA, SEIZURES	BILATERAL	SUPRATENTORIAL REGION	MULTIPLE	ILL DEFINED	-	ISOINTENSE	HYPERINTENSE	ABSENT DIFFUSION RESTRICTION	-	NORMAL	ENCEPHALITIS
34	SANTOSH KUMBAR	18	M	HEADACHE, VOMITING, ATAXIA	BILATERAL	SUPRATENTORIAL, BRAINSTEM AND INFRATENTO	MULTIPLE	WELL DEFINED	-	HYPOINTENSE	HYPERINTENSE	PERIPHERAL RESTRICTION	RING ENHANCEMENT	AA peak, iTre	FUNGAL ABSCESS
35	SAVANT BANAKR	38	M	FEVER, VOMITING, MOTOR WEAKNESS	BILATERAL	SUPRATENTORIAL	MULTIPLE	ILL DEFINED	+	ISOINTENSE	HYPOINTENSE	ABSENT DIFFUSION RESTRICTION	-	rNAA	HIV ENCEPHALITIS
36	SEVANTI ABBIGERI	21	F	HEADACHE, FEVER, ALTERED SENSORIUM	BILATERAL	FRONTAL, PARIETAL AND OCCIPITAL REGIONS	MULTIPLE	ILL DEFINED	+	ISOINTENSE	HYPERINTENSE	DIFFUSION RESTRICTION	N/A	NORMAL	ENCEPHALITIS
37	SHEETAL RAMAOGDE	26	F	HEADACHE, FEVER, ALTERED SENSORIUM	BILATERAL	FRONTAL, PARIETAL AND OCCIPITAL REGIONS	MULTIPLE	WELL DEFINED	-	ISOINTENSE	HYPOINTENSE	PERIPHERAL RESTRICTION	PERIPHERAL ENHANCING	LL PEAK, r NAA, rNAA/Cr	TUBERCULOMA WITH MENINGITIS
38	SHIVAM JADHAV	28	M	HEADACHE, FEVER, SEIZURES	BILATERAL	FRONTAL , PARIETAL AND OCCIPITAL REGIONS	MULTIPLE	WELL DEFINED	+	NORMAL	NORMAL	ABSENT DIFFUSION RESTRICTION	LEPTOMENINGEAL AND EPEN	NORMAL	MENINGITIS WITH VENTRICULITIS
40	SHOBHA DESAI	60	F	HEADACHE, FEVER, VOMITING	BILATERAL	FRONTOPARIETAL REGIONS, CEREBELLAR LOBES	MULTIPLE	WELL DEFINED	-	ISOINTENSE	HYPERINTENSE	DIFFUSION RESTRICTION	RING ENHANCING	LL PEAK, rNAA/Cr	TUBERCULOMA WITH MENINGITIS
39	SHOBHA UPPAR	46	F	FEVER, VOMITING	BILATERAL	BASAL GANGLIA, TEMPORAL REGION, PONS, CERE	MULTIPLE	WELL DEFINED	-	ISOINTENSE	HYPERINTENSE	DIFFUSION RESTRICTION	ENHANCING	rNAA, iCho	PML
41	SHRADHHA GARGATTI	36	F	HEADACHE, FEVER, VOMITING	LEFT	TEMPORAL REGION, GYRI IN PARITO-TEMPORAL	1	WELL DEFINED	-	ISOINTENSE	ISOINTENSE	ABSENT DIFFUSION RESTRICTION	FOCAL AND LEPTOMENINGEA	LL PEAK, rNAA/Cr	TUBERCULOMA WITH MENINGITIS (
42	SHRINIVAS HARIDAS	62	M	HEADACHE	BILATERAL	BASAL GANGLIA AND FRONTOPARIETAL REGION	MULTIPLE	WELL DEFINED	-	HYPOINTENSE	HYPERINTENSE	PERIPHERAL RESTRICTION	RING ENHANCING	LL peak	TUBERCULAR ABSCESS
43	SUDHA PATANGE	52	F	HEADACHE, VOMITING	BILATERAL	TEMPORAL REGIONS, LEFT INSULAR CORTEX AND	MULTIPLE	WELL DEFINED	-	HYPOINTENSE	HYPOINTENSE	PERIPHERAL RESTRICTION	RING ENHANCING	LL peak	TUBERCULOMA
44	SUMAN HONAGEKAR	42	F	HEADACHE, FEVER, VOMITING	BILATERAL	FRONTAL AND PARIETAL, CSO AND CR	MULTIPLE	WELL DEFINED	-	HYPOINTENSE	HYPERINTENSE	ABSENT DIFFUSION RESTRICTION	N/A	rNAA, iCho, iLac, iLip	PML
45	SURESH TORASA	43	M	HEADACHE, FEVER, VOMITING, ATAXIA	LEFT	BASIFRONTAL REGION	MULTIPLE	ILL DEFINED	-	HYPOINTENSE	HYPERINTENSE	DIFFUSION RESTRICTION	ENHANCING	rNAA, rNAA/Cr ratio	CEREBRITIS
46	VIJETHA MOHITHE	41	F	WEIGHT LOSS, HEADACHE	BILATERAL	SUPRATENTORIAL AND INFRATENTORIAL REGION	MULTIPLE	ILL DEFINED	+	ISOINTENSE	HYPER INTENSE	ABSENT DIFFUSION RESTRICTION	N/A	rNAA	HIV ENCEPHALITIS
47	VINOD KARI	19	M	FEVER, VOMITING	LEFT	FRONTAL REGION	1	WELL DEFINED	-	HYPOINTENSE	HYPERINTENSE	PERIPHERAL RESTRICTION	PERIPHERALENHANCING	iAc, LL peak, iGly,	BACTERIAL ASBSCESS
48	YALLUBAI SHINDOLKAR	65	F	HEADACHE, FEVER, VOMITING	RIGHT	PONS	1	WELL DEFINED	-	ISOINTENSE	HYPERINTENSE	ABSENT DIFFUSION RESTRICTION	PERIPHERAL ENHANCING	iAc, LL peak, iGly, iA/S ratio	BACTERIAL ASCESS